



Calhoun: The NPS Institutional Archive
DSpace Repository

Theses and Dissertations

1. Thesis and Dissertation Collection, all items

1973

Design, construction and testing of a high voltage pulsed regulator for use in the NPS linear accelerator.

Skiano, Ralph Dennis.

Monterey, California. Naval Postgraduate School

<http://hdl.handle.net/10945/16556>

Downloaded from NPS Archive: Calhoun



Calhoun is the Naval Postgraduate School's public access digital repository for research materials and institutional publications created by the NPS community. Calhoun is named for Professor of Mathematics Guy K. Calhoun, NPS's first appointed -- and published -- scholarly author.

Dudley Knox Library / Naval Postgraduate School
411 Dyer Road / 1 University Circle
Monterey, California USA 93943

<http://www.nps.edu/library>

DESIGN, CONSTRUCTION AND TESTING OF A
HIGH VOLTAGE PULSED REGULATOR
FOR USE IN THE NPS LINEAR ACCELERATOR

Ralph Dennis Skiano

Library
Naval Postgraduate School
Monterey, California 93940

NAVAL POSTGRADUATE SCHOOL

Monterey, California



THESIS

Design, Construction and Testing of a
High Voltage Pulsed Regulator
for Use in the NPS Linear Accelerator

by

Ralph Dennis Skiano

Thesis Advisors:

E.B. Dally
G.D. Ewing

June 1973

Approved for public release; distribution unlimited.

Design, Construction and Testing
of a
High Voltage Pulsed Regulator
for
Use in the NPS Linear Accelerator

by

Ralph Dennis Skiano
Ensign, United States Navy
B.E.E., Villanova University, 1972

Submitted in partial fulfillment of the
requirements for the degree of

MASTER OF SCIENCE IN ELECTRICAL ENGINEERING

from the
NAVAL POSTGRADUATE SCHOOL
June 1973

ABSTRACT

This paper describes the design, construction and testing of a pulsed high voltage regulator installed in one modulator of the Naval Postgraduate School Linear Accelerator. The design is adapted from a similar network in use at Stanford University. The prototype system was found to improve the voltage regulation by a factor of 168, and to eliminate undesirable energy shifts in the electron beam due to fluctuations in line voltage.

TABLE OF CONTENTS

I.	INTRODUCTION -----	9
	A. BACKGROUND TO THE PROBLEM -----	9
	B. SURVEY OF APPROACHES TO THE SOLUTION -----	11
	C. THE SOLUTION AND A BRIEF DESCRIPTION OF THE SYSTEM -----	16
II.	DESIGN OF THE SYSTEM -----	20
	A. THEORETICAL DESIGN -----	20
	1. Theoretical Analysis and Design of the De-Q'ing System -----	20
	2. Theoretical Analysis and Design of the Voltage Divider -----	32
	B. EMPIRICAL DESIGN -----	37
	1. The Comparator Circuit -----	37
	2. The Trigger Chassis -----	40
	a. Description of a Thyatron -----	40
	b. Trigger Circuit Requirements -----	42
	c. General Principle Behind the Trigger Circuit -----	43
	d. Operation of the Trigger Circuit -----	45
III.	CONSTRUCTION OF THE PROTOTYPE -----	53
	A. CONSTRUCTION OF THE DE-Q'ING BRANCH -----	53
	B. CONSTRUCTION OF PULSE TRANSFORMERS -----	57
	C. CONSTRUCTION OF THE REMAINDER OF THE PROTOTYPE	59
	D. CONSTRUCTION OF THE R-C COMPENSATED VOLTAGE DIVIDER -----	59
IV.	TESTING OF THE PROTOTYPE -----	62

A. TESTS PRIOR TO PROTOTYPE INSTALLATION -----	62
B. TESTING OF THE PROTOTYPE -----	67
1. Preliminary Problems and Circuit Changes	67
2. Other Circuit Changes -----	72
3. Measuring Improvement Factor Due to Prototype -----	72
APPENDIX A. Derivation of Equation (8) -----	79
APPENDIX B. Alternative Method of Compensation -----	81
BIBLIOGRAPHY -----	84
INITIAL DISTRIBUTION LIST -----	85
FORM DD 1473 -----	86

LIST OF FIGURES

1.	Simple Diagram of One Modulator -----	12
2.	Explanation of Resonance Charging -----	13
3.	Simplified Diagram of Charging Network with De-Q'ing Circuit -----	17
4.	Waveforms Associated with Figure 3 -----	18
5.	Overall Block Diagram of Pulse Regulator -----	21
6.	Analysis of De-Q'ing Branch -----	23
7.	Compensated De-Q'ing Signal Divider Waveforms -----	34
8.	Final Circuit Diagram of the Comparator Circuit ---	31
9.	Principle Behind the Trigger Circuit -----	44
10.	Circuit Diagram of Trigger Chassis and Output Pulse Transformer -----	46
11.	Anode Voltage Waveforms in the Trigger Chassis ----	50
12.	Open-Circuit Generated Pulses -----	51
13.	Grid Pulse Triggering De-Q'ing Thyatron -----	52
14.	Miscellaneous Circuitry Constructed -----	56
15.	Physical Layout of De-Q'ing Branch -----	58
16.	Rough Sketch of Approximate Physical Layout of Prototype System -----	60
17.	Present High Voltage Monitors at Control Panel ----	63
18.	Chart Recordings of Typical Variations in V_{DC} -----	65
19.	Clipped Charge Waveform and Comparator Output -----	70
20.	$V_{DC} + v_L$ for Different Values of C -----	73
21.	$V_{DC} + v_L$ for $C = .5\mu f$ -----	74
22.	De-Q'ing System: Final Schematic -----	76

23.	Simple Diagram of Relationship of Beam Intensity to Klystron Voltage -----	78
24.	Explanation of Alternate Type of Compensation ---	82



LIST OF TABLES

I. Design Parameters for De-Q'ing Branch -----	32
--	----

ACKNOWLEDGEMENTS

I would like to express my gratitude to the following people who helped in the completion of this project.

First, Dr. Gerald D. Ewing, Professor of Electrical Engineering and Edgar B. Dally, Professor of Physics, were a constant source of knowledge and encouragement. Frederick R. Buskirk, Professor of Physics, provided most of the early direction in the approach to the problem. William T. Tomlin of the Stanford Linear Accelerator Center provided the author with the benefits of his personal experience with the de-Q'ing circuit. Harold L. McFarland and Donald D. Snyder built all of the parts of the system and provided much practical knowledge of the hardware involved. My wife, Peggy typed the first manuscript, did all of the drawings, and generally provided much support throughout the duration of the project.

Finally, I would like to thank Jesus Christ for guiding me to the completion of this project through all of the above-mentioned people.

I. INTRODUCTION

This paper concerns the problem of and solution for the regulation of pulsed high voltage for klystrons of the linear electron accelerator (LINAC) at the Naval Postgraduate School (NPS).

A. BACKGROUND TO THE PROBLEM

The LINAC is a thirty foot long cylindrical disc-loaded waveguide. When microwave energy of the proper frequency is propagated down the waveguide, a part of each cycle of the travelling wave has its electric field directed axially and is moving at the speed of light. Electrons which are injected into the structure, at or near the velocity of light, are accelerated by this axially-directed field. Since the electrons remain in a constant phase relationship, the electrons can experience an accelerating force for the entire length of the LINAC, thus increasing their energy from a comparatively small initial value to a large final value.¹

The final energy of the accelerated electrons is proportional to the square root of the product of the total

¹Stanford University Microwave Laboratory Report 173, Pulsers for the Stanford Linear Electron Accelerators, Nov. 1952, p. 1.

power and the length of the waveguide.² At NPS, the maximum energy is about 108 million electron volts (MeV). In order to achieve this, the LINAC is divided into three ten-foot sections, and each section is supplied with seventeen megawatts (MW) peak power. The power is obtained from individual high power klystron amplifier tubes.

The input power required to each of the three klystrons is 125 MW. On a continuous input power basis, the resulting input power need of 375 MW would be completely out of the question. Therefore, the input power to the klystron amplifiers is pulsed; that is, the equipment is turned on for a short period of time (two microseconds (μ s) in this case), and then allowed to rest (for 1/60 of a second). The duty cycle (time-on divided by total time available) is thus .00012, and this reduces the average input power requirement per klystron to 15 kilowatts (kW).

The pulsing is accomplished by charging a pulse forming network (PFN) to a working voltage and discharging it to the klystron using a thyatron switch. This system is called the modulator and there is one modulator for each klystron. The pulses have a peak voltage of approximately 220 kV and they are delivered to the cathode of the klystron through a pulse transformer, turning the klystron on for 2 μ s. The accuracy of many of the electron-scattering experiments done with the LINAC depends on the steadiness

²Ibid, p. 2.

of the amount of energy given to the electrons each cycle. This energy depends on the output power of the klystron during the "on" time of the cycle. It is known that this output power depends in turn on the amplitude of the beam voltage in the klystron.

If the energy imparted to the electrons fluctuates from cycle to cycle, this results in energy shifts of the beam as well as reduced beam intensity. For large shifts, i.e., if the amount of energy in a given pulse deviates beyond a limiting point, the entire beam is "lost" and the high voltage must be readjusted by the operator. Although there were other causes of pulse-to-pulse energy deviation, the main cause was the pulse-to-pulse voltage fluctuation on the klystron. Figure 1 shows the basic components of the modulator. The problem was attacked by attempting to hold constant the peak voltage built up on the PFN.

B. SURVEY OF APPROACHES TO THE SOLUTION

Figure 2(a) shows a simplified diagram of the charging network. The principle of this network is the well-known "resonance charging"; i.e., using the high-Q of the effective L-C network to effectively double the voltage from the supply. Figure 2(b) shows the voltage waveform across the PFN. Without the charging diode, the circuit would oscillate at its natural frequency $1/(LC_{\text{PFN}})^{1/2}$, and the amplitude of the voltage would be $2V_{\text{DC}}$ as shown in the dotted lines of the figure. The inductor would initially begin

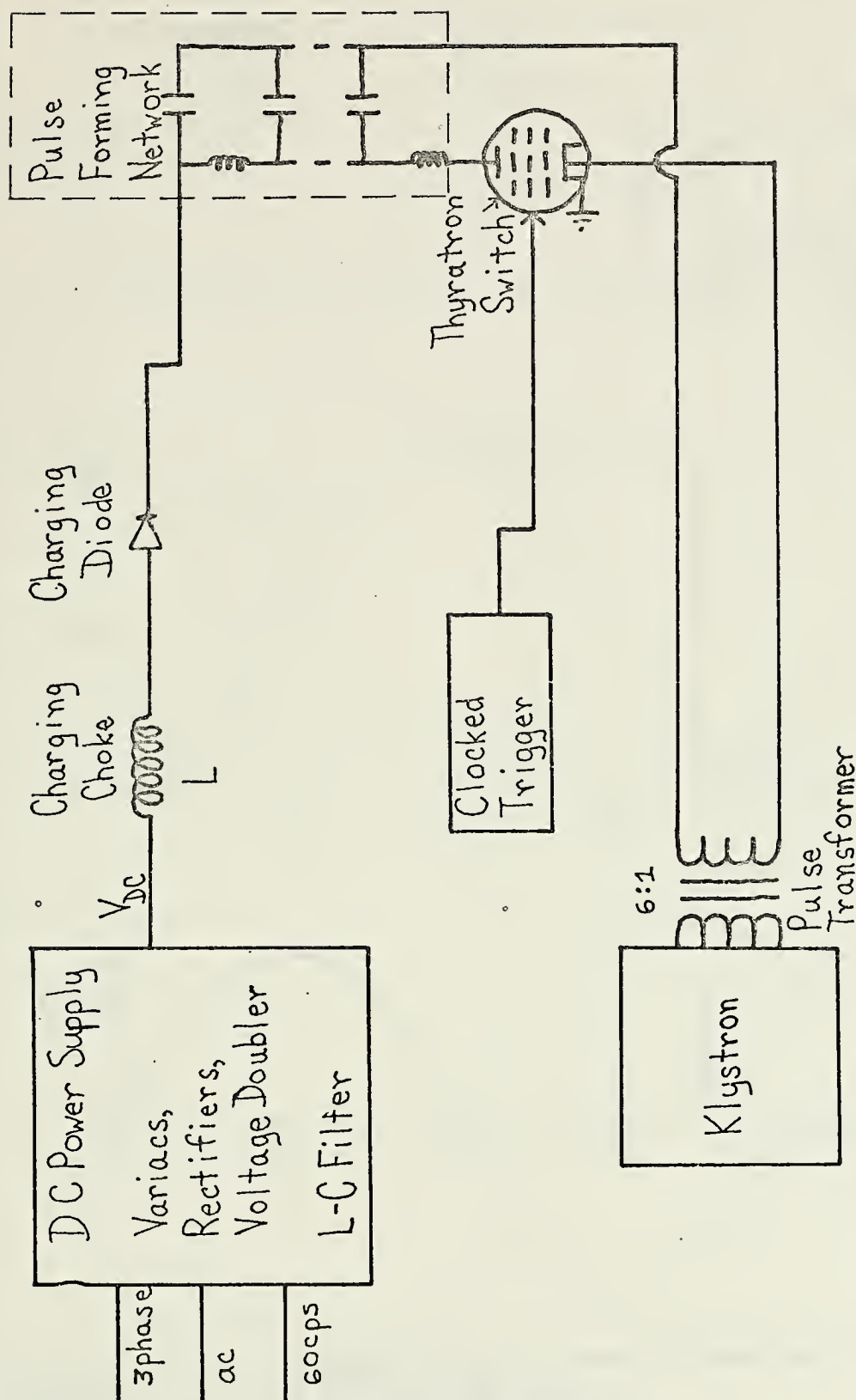


FIGURE 1 - SIMPLE DIAGRAM OF ONE MODULATOR

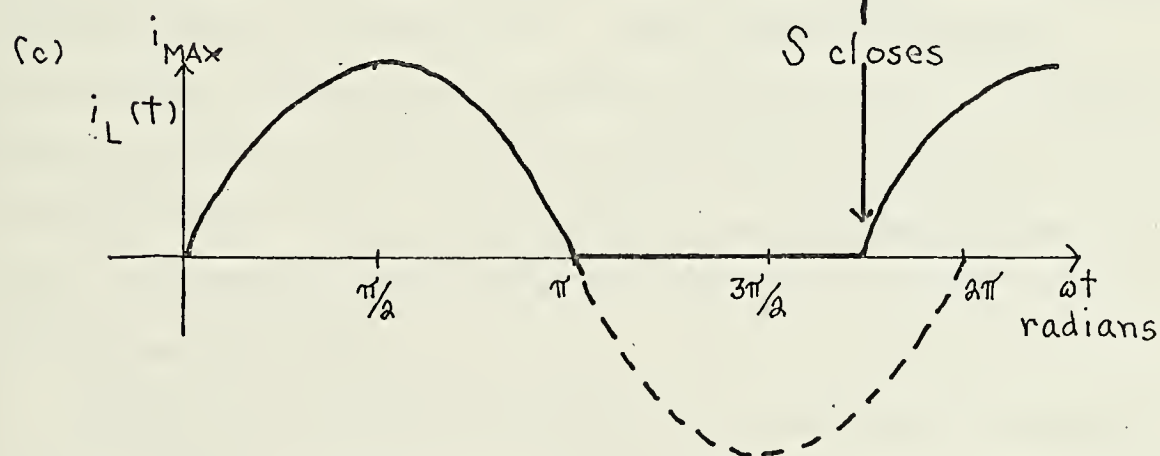
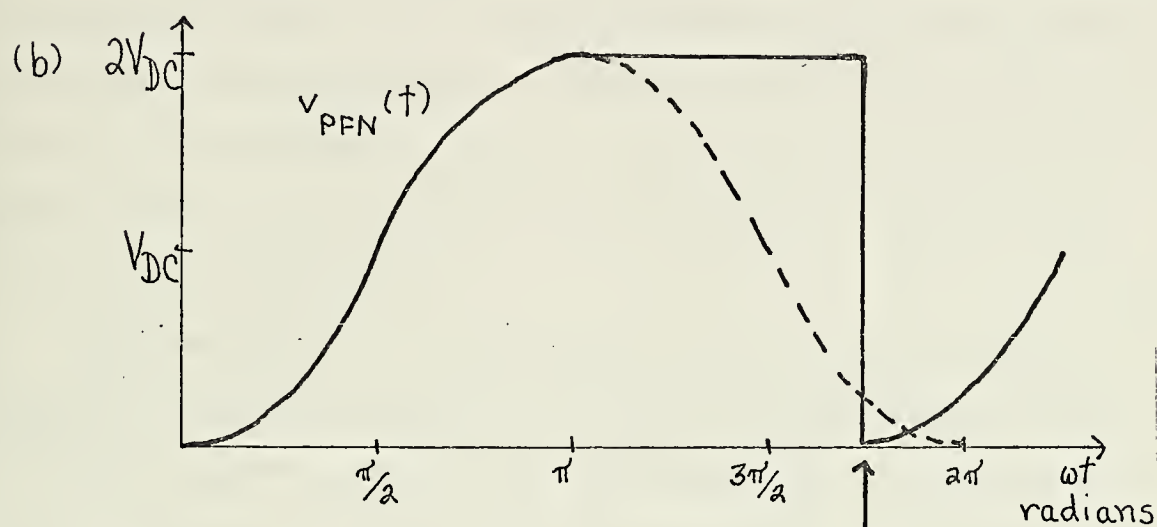
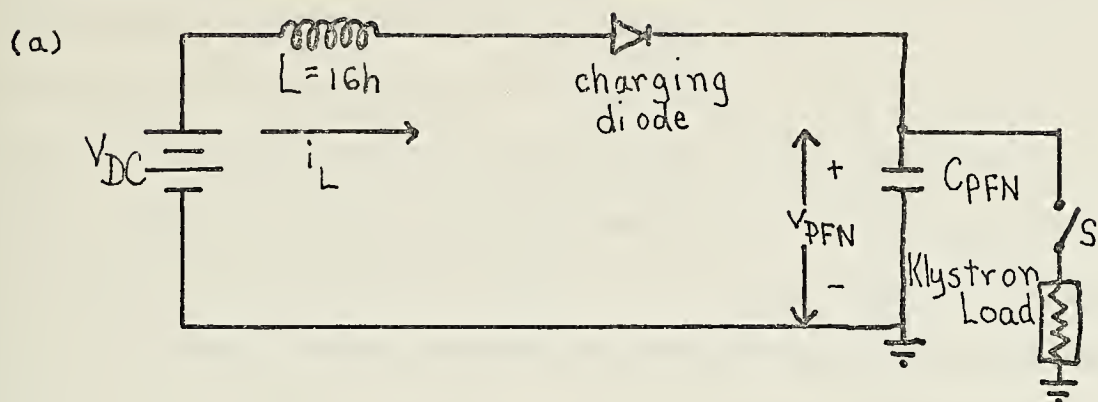


FIGURE 2- (a) Simplified diagram of charging network
 (b) PFN voltage vs. ωt
 (c) Inductor current vs. ωt

to store energy, as would the capacitor, until $\omega t = \pi/2$, at which point the inductor would begin to act like a source and dump its energy into the capacitor. Thus, by $\omega t = \pi$ the current is zero and the voltage across the capacitor is $2V_{DC}$, and there is no energy left in L. However, with the series charging diode present, the current may not reverse its direction; thus, instead of seeing the capacitor discharge into the inductor (as would normally happen) and the oscillations occur, the current remains zero, and the PFN capacitor remains charged up until switch S is closed and then all the energy in C_{PFN} is dumped into the klystron load. At that point, the network begins to recharge and the cycle is repeated.

One can see that if V_{DC} varies for any reason, then V_{PFN} will not be constant. At first it was thought that the best way to solve the problem would be to regulate V_{DC} . However, V_{DC} is a very large voltage. It is generally between sixteen and twenty kV. Some type of threshold device like a zener diode, which works well at low voltages, was at first considered, but it would have required a prohibitively long string of them to provide regulation. Also, the current which would have had to be diverted was in the ampere region.

Another idea to try to control V_{DC} was to use a chopped or pulsed sinusoid at the input to the dc power supply. It was really a gated sinusoid and by varying the duty cycle of the pulse train applied to the gate, the average ac

power fed into the supply could be very accurately controlled, and thus so could V_{DC} . However, the output of the power supply contains a large inductor and the usual filter capacitor. It was not desired to face the high voltage problems associated with instantaneously stopping and starting current in that inductor.

Another possibility was to try to regulate the ac all the way back at the input transformers. There are devices which do this magnetically within the transformer. However, a magnetic system is inherently slow (even for sixty-cycle operation), and a transformer of the type needed would have been too costly and not accurate enough.

Another way to regulate ac was to use feedback from the sampled signal to small electric servo-motors connected mechanically to the variacs which control the amount of incoming ac. However, this was felt to be too slow and lack sufficient accuracy, and also to have inherent stability problems.

The problem could therefore not be treated as a normal case of ac or dc regulation, but each pulse had to be monitored and regulated. Since the mode of operation was already pulsed, the controller had to be pulsed also. What was needed was an alternate path to switch the current from the inductor once the desired value of v_{PFN} had been reached. Then, this "threshold" could be set lower than the lowest expected variation of working voltage and the "alternate path" could handle the remaining current in the choke.

This, of course, would be amplitude-controlled and would be able to regulate on each individual pulse.

Much work had already been done and the problem had been solved by a number of other people involved in LINAC design. The purpose of this project was to adapt the design to the NPS LINAC and to construct a regulation system for the high voltage modulator.

C. THE SOLUTION AND A BRIEF DESCRIPTION OF THE SYSTEM

As will be discussed later in the paper, the best method to accomplish the necessary regulation has been to use a low-Q tank circuit as the alternate path. The process of switching from the high-Q to a low-Q circuit is what gives the circuit its name: "de-Q'ing". Figures 3 and 4 show the general layout of the original design, as well as the important waveforms. In essence, the voltage V_{PFN} is held at the trigger value by keeping the charging diode reverse-biased while dissipating the remaining choke energy in resistor R. The analysis and construction of such a circuit will be the subject of this thesis.

Because of the high voltages involved and the speed at which the switch must be made, it was decided to use hydrogen thyratrons as switches. They are faster, and handle higher voltages than SCR's. There was also a surplus stock of them on hand, so economically they were very desirable. Finally, although they are physically large, there was enough space for them and the required insulation within the confines of the high voltage cage.

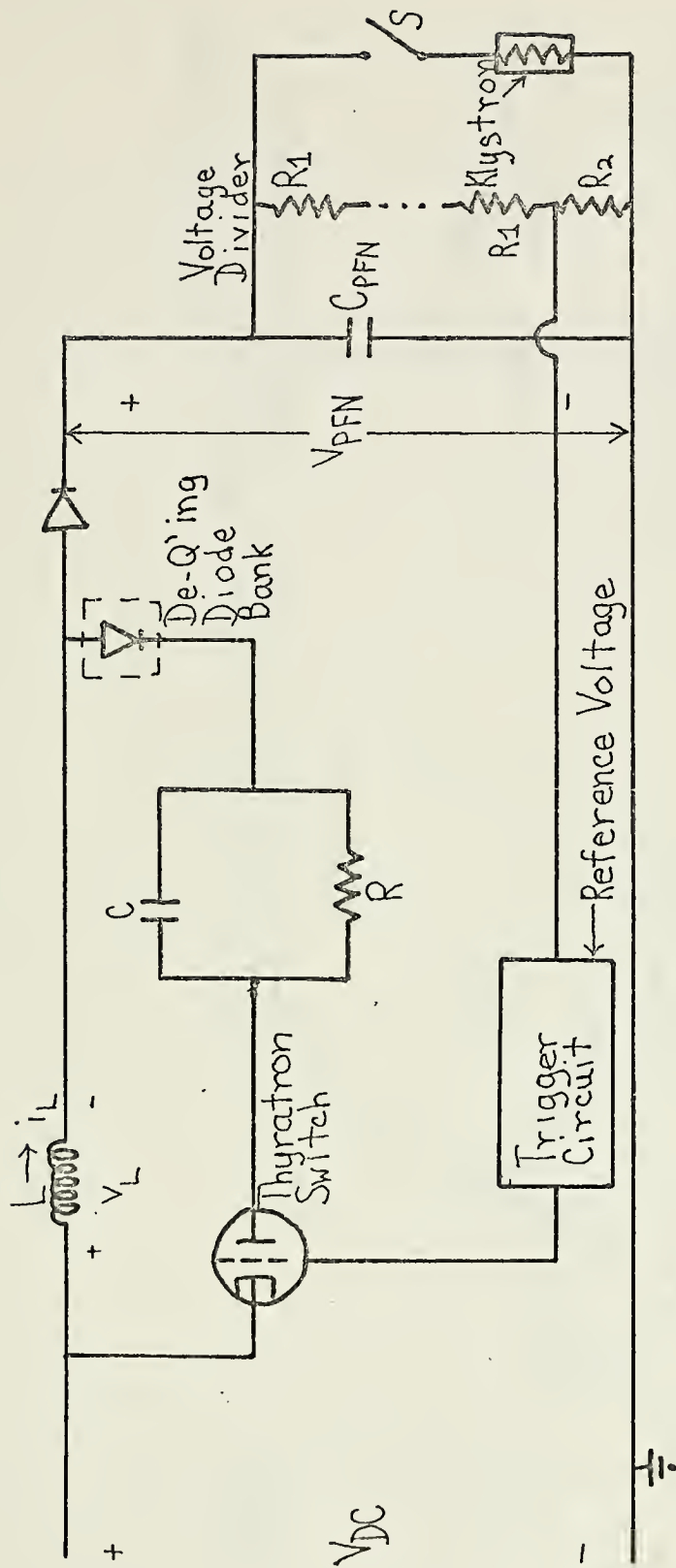


FIGURE 3-SIMPLIFIED DIAGRAM OF CHARGING NETWORK WITH DE-Q'ING CIRCUIT

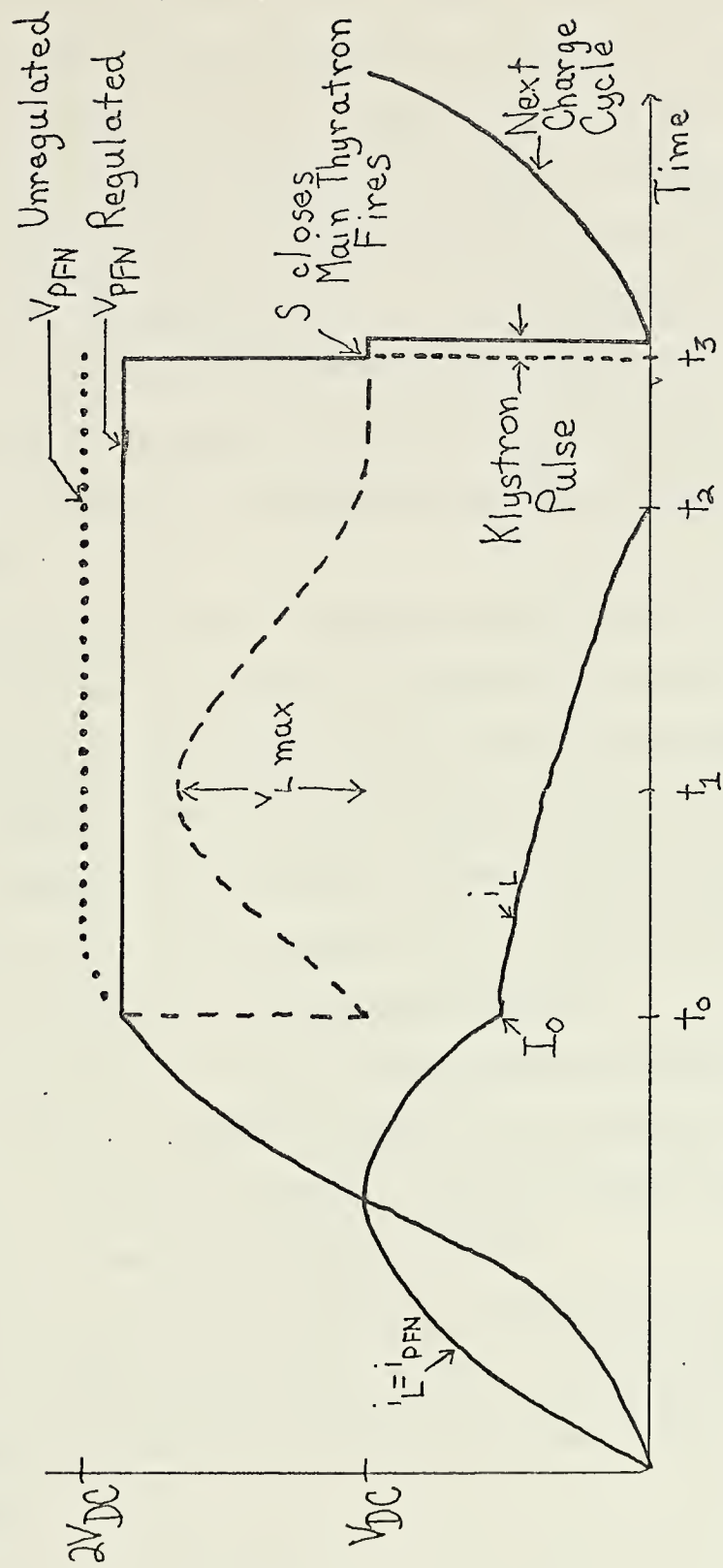


FIGURE 4-WAVEFORMS ASSOCIATED WITH FIGURE 3

Briefly, the other parts of the system will now be mentioned. They will be discussed more thoroughly later in the paper. The trigger circuit triggers the de-Q'ing thyatron when the proper reference voltage is reached. The purpose of this circuit is to generate a 1500 volt spike on the grid of the thyatron, as the sampled PFN voltage begins to surpass the reference voltage. The forty kV insulation which is necessary between the trigger circuit and the grid is provided by immersing the pulse transformer in an oil bath.

Another component in the original design was a compensated voltage divider, intended to compensate for the firing delay by introducing the proper phase shift in the sample of the PFN voltage it fed into the trigger circuit. During testing, however, this divider caused severe problems and eventually it had to be replaced by a resistive divider situated on the PFN side of the charge diodes.

Although not shown in Fig. 3, the comparator was the actual place where the sampled signal and reference voltage were compared. This had to have a very high input impedance so as not to load the voltage divider.

The system also includes supplies and support equipment for the de-Q'ing thyatron, as well as a large diode string necessary to make the alternate current path unidirectional.

II. DESIGN OF THE SYSTEM

The method of designing the system was varied because certain parts of the system were more amenable to theoretical analysis than others. For the purposes of this paper, theoretical design refers to those parts of the system which were designed completely on paper and installed in the prototype without any prior testing. Empirical design refers to those subsystems that were not rigorously analyzed, although some calculations were made to determine initial component values. Before they were installed in the prototype, they were pretested on a breadboard and modified until they operated sufficiently well.

A. THEORETICAL DESIGN

The overall system block diagram is given in Fig. 5. Of the several pieces of equipment involved, only two were completely analyzed on a theoretical basis. They are the de-Q'ing path and the compensated voltage divider.

1. Theoretical Analysis and Design of the De-Q'ing Branch

The de-Q'ing branch consists of a hydrogen thyatron, a diode bank, and a parallel combination of resistors and capacitors whose purposes are to: (1) reverse-bias the charging diodes; and (2) dissipate all remaining energy in L before the start of the next pulse in response to a

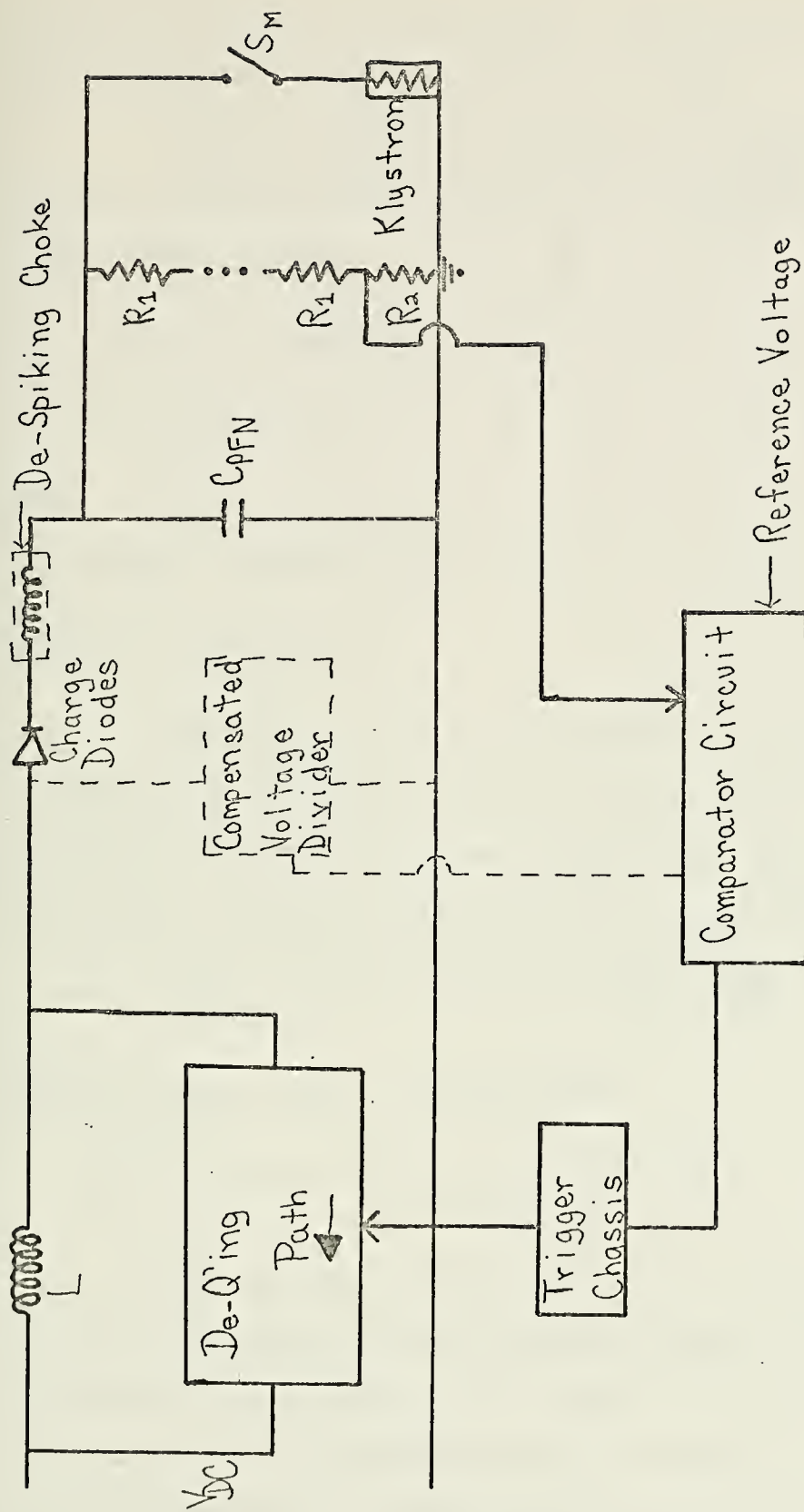


FIGURE 5-OVERALL BLOCK DIAGRAM OF PULSE
REGULATOR

command generated by the trigger chassis when the sampled PFN voltage reaches the reference voltage.

Figure 2 shows the unregulated PFN voltage and current waveforms that, for $0 \leq \omega t \leq \pi$, are described by the following equations

$$v_{\text{PFN}} = V_{\text{DC}}(1 - \cos \omega t), \quad (1)$$

$$v_L = -V_{\text{DC}} \cos \omega t, \quad (2)$$

and

$$i_{\text{PFN}} = (V_{\text{DC}}/\omega L) \sin \omega t = i_L, \quad (3)$$

where $\omega = (LC_{\text{PFN}})^{-1/2}$.

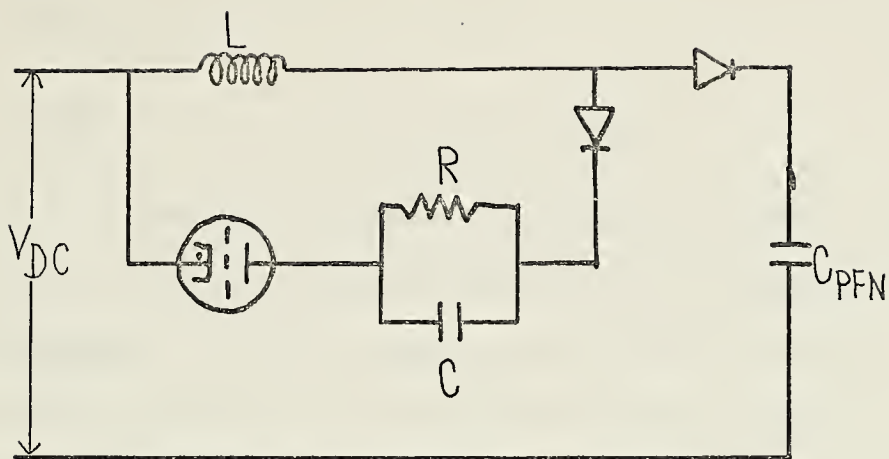
Figure 6 shows the system with de-Q'ing as well as the equivalent circuit of the de-Q'ing path. Let $I_0 = i_L(t_0)$. Then if the switch is thrown at time t_0 , the integro-differential equation describing the action is given as

$$-I_0 + \frac{1}{L} \int_{t_0}^t v_L(\tau) d\tau + \frac{1}{R} v_L(t) + C dv_L \frac{(t)}{dt} = 0,$$

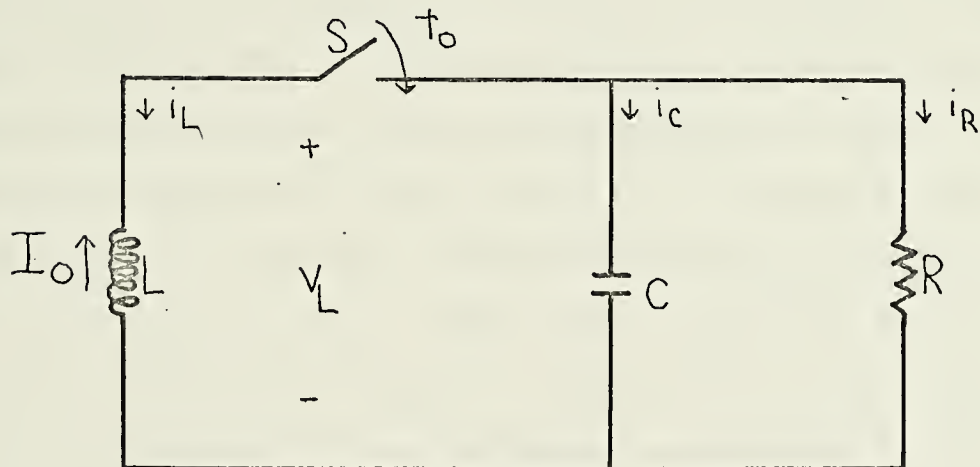
which becomes, after manipulation

$$v_L(t) + RC \dot{v}_L(t) + \frac{R}{L} \int_{t_0}^t v_L(\tau) d\tau = RI_0. \quad (4)$$

This equation can be reduced to a second order differential equation which can have one of three possible solutions, depending upon the choice of R, L, and C. (For the reader who is unfamiliar with a method for solving this equation, Appendix A contains a Laplace transform approach to the solution.) The three possible solutions are related



(a) De-Q'ing components in place



(b) Equivalent circuit of de-Q'ing path

FIGURE 6

to the roots of the characteristic equation derived from the differential equation. The discriminant of the characteristic equation is

$$\left(\frac{1}{RC}\right)^2 - \frac{4}{LC}.$$

If this term is positive, the characteristic equation will have real, distinct roots and the response is termed overdamped. If this term is zero, the roots are equal and the response will be of the form $(C_1 + C_2 t)e^{\alpha t}$, and is known as critically damped. If the term is negative, the roots become complex conjugates and the response is termed underdamped or damped oscillatory.

The value of L is fixed at 16 henries. The question facing the designer was what type of response would fulfill the two purposes of the de-Q;ing branch. To answer this question it was necessary to determine what these purposes mean quantitatively. The first purpose, to reverse-bias the charging diodes, means that the maximum v_L after the switch closes must be less than $v_L(t_0^-)$. Suppose one wanted to clip the pulse 10% from its unregulated peak, i.e., at $v_{PFN} = 1.8V_{DC}$. This would require the maximum v_L to be less than or equal to $.8V_{DC}$. The largest V_{DC} available is 20kV. Thus, it would be desirable to keep $v_{L \max}$ less than 16kV. However, the normal operating value of V_{DC} is around 18kV, which would imply that $v_{L \max}$ be kept less than 14.4kV. Allowing a safety factor (or margin of error) of about 1.5, this would reduce the value of

$v_{L \max}$ even further, to 10kV. So, somewhat arbitrarily, the first purpose of the de-Q'ing branch can be restated as

$$v_{L \max} \leq 10\text{kV}. \quad (5)$$

The second purpose concerns time. If the de-Q'ing thyatron is fired at time t_0 (see Fig. 4), and the energy in L is finally zero at time t_2 , then the time $(t_2 - t_0)$ may be considered the response time of the de-Q'ing branch. The requirement that all energy in L is dissipated before the start of the next pulse may be stated in terms of Fig. 4 as $t_2 - t_0 \leq t_3 - t_0$. The total time from the beginning of one charge cycle to the next (t_3) is given by $1/\text{PRR}$, where PRR is the pulse repetition rate, in this case 60pps. Thus, $t_3 \approx 16.7\text{ms}$. The voltage at which the pulse is to be clipped is assumed to be within 10% of the unregulated peak and thus, ωt_0 will always be between 2.5 and π radians (i.e. $\cos^{-1}(-.8)$ and $\cos^{-1}(-1)$). Now, $C = .375\mu\text{f}$, and $L = 16\text{H}$, so $\omega = 410$. This places the time of firing, t_0 roughly between 9.0 and 10.6 ms. Using the lower limit, the second purpose now can be restated as

$$t_2 - t_0 \leq 9\text{ms}. \quad (6)$$

With relations (5) and (6) as constraints, one can begin to choose the form of the solution to (4). An overdamped solution was investigated but due to the strong dependence on the exponential nature of this solution, the response time was too long. The same thing was true of a

critically damped solution. Because the diode action maintains current flow unidirectional, however, a damped oscillatory solution proved to be most promising. That is, the damped frequency could be chosen to satisfy requirement (6), while the exponential factor would handle (5).

If the damped frequency of the network is defined as ω_0 , then from Eq. (4) it can be shown (see Appendix A) that

$$\omega_0 = \sqrt{1/LC - 1/4R^2C^2} \quad (7)$$

and

$$v_L(t) = \frac{I_0}{\omega_0 C} \exp \frac{-\omega_0(t-t_0)}{2\omega_0 RC} \sin \omega_0(t-t_0). \quad (8)$$

This voltage is the voltage across the de-Q'ing branch after the thyatron fires. Note that the initial effect of the switch action is to reduce v_L to zero. Physically, this occurs because the uncharged capacitor C initially acts as a short circuit, and this initial sharp drop in voltage insures that the conduction of current to the PFN ceases. The capacitor then charges up to some maximum value, $v_{L \max}$, and eventually it and the inductor dissipate all their energy in R. (See Fig. 4.) The broken-line waveform shows the voltage at the anode of the charging diode, $v_L + V_{DC}$.

The system requirement given by Eq. (5) is recalled, and $v_{L \max}$ must be computed. This is done by equating the time derivative of Eq. (8) to zero, and the resulting equation is

$$v_{L \max} = I_0 R \left[2 \exp \frac{-\omega_0(t_1 - t_0)}{\tan \omega_0(t_1 - t_0)} \cos \omega_0(t_1 - t_0) \right], \quad (9)$$

where t_1 is the time at which the peak occurs. This maximum occurs when $2\omega_0 RC = \tan \omega_0(t_1 - t_0)$.

Another important quantity is the inductor current which is diverted from the PFN. This current, $i_L(t)$, is found by integrating $v_L(t)$ from t_0 to t and is given by

$$i_L(t) = I_0 \exp \frac{-\omega_0(t - t_0)}{2\omega_0 RC} \frac{\sin[\omega_0(t - t_0) + \omega_0(t_1 - t_0)]}{\sin \omega_0(t_1 - t_0)}. \quad (10)$$

Note that at $t = t_0$, i_L reduces I_0 as expected. It is desired that the current in the choke be zero at the start of the next charge cycle. The waveform (see Fig. 4) is a damped sinusoid and will pass through zero at $\omega_0(t - t_0) + \omega_0(t_1 - t_0) = \pi$. When this happens, the current will try to reverse but the unidirectional nature of the thyatron and the diodes will prevent this from happening and the choke current will remain at zero. To insure that this occurs before the start of the next charge cycle, referring to Fig. 4, ω_0 must be selected so that³

$$\omega_0(t_3 - t_0) + \omega_0(t_1 - t_0) \geq \pi. \quad (11)$$

At this point it is convenient to begin to think of the circuit in terms of its Q , i.e., the ratio of energy

³William Tomlin, "Pulse Forming Network Voltage Regulation," in The Stanford Two-Mile Linear Accelerator, R.B. Neal, et. al. eds. New York, 1968, p. 430.

stored to energy dissipated. For the circuit in question⁴

$$Q = \omega_N RC = RC/\sqrt{LC} = R\sqrt{C/L} \quad . \quad (12)$$

From Eqs. (7) and (11) one can write

$$\omega_0 RC = \sqrt{R^2 C/L - 1/4} = \sqrt{Q^2 - 1/4} = \sqrt{\frac{4Q^2 - 1}{2}}$$

or

$$2\omega_0 RC = \sqrt{4Q^2 - 1} \quad . \quad (13)$$

It can also be shown that

$$C = (1 - 1/4Q^2)/\omega_0^2 L, \quad (14)$$

and from the maximization condition necessary for Eq. (9), it follows that the proper R should be chosen to satisfy

$$R = \frac{\tan \omega_0 (t_1 - t_0)}{2\omega_0 C} \quad . \quad (15)$$

The purpose of the previous mathematical work has been to lay the groundwork for choosing the proper values of R and C and for making other engineering decisions regarding parameters. There are four other quantities left to investigate before the design procedure will be discussed.

The first is power dissipation in the resistor bank. The power dissipation is given by

⁴William Tomlin, personal interview at Stanford Linear Accelerator Center, Stanford, California, March 1973.

$$P = \frac{LI_0^2}{2} \text{ PRR.} \quad (16)$$

The average current expected through the thyatron is significant since although most thyatrons are rated with high peak currents, their average and root-mean-square current ratings are fairly low. The average current can be calculated by integrating Eq. 10 as⁵

$$I_{\text{switch}}(\text{AV}) = \frac{\text{PRR}}{\omega} \int_0^{\pi - \omega_0(t_1 - t_0)} i_L(t) d(\omega_0 t).$$

The upper limit of integration is found by solving Eq. (10) for the angle $\omega_0(t_2 - t_0)$ at which the current becomes zero. This will always be in the second quadrant and can thus be written as $\omega_0(t_2 - t_0) = \pi - \omega_0(t_1 - t_0)$. The lower limit is the angle $\omega_0 t_0$ when the de-Q'ing circuit is fired and represents zero on the $\omega_0 t$ scale. Carrying out the integration yields⁶

$$I_{\text{switch}}(\text{AV}) = (\text{PRR}) I_0 (\text{LC}_{\text{PFN}})^{1/2} \left\{ \exp - \frac{\pi - \omega_0(t_1 - t_0)}{\tan \omega_0(t_1 - t_0)} \right. \\ \left. \times \sin \omega_0(t_1 - t_0) + \sin 2\omega_0(t_1 - t_0) \right\}. \quad (17)$$

The rms current can be approximated by calculating the current for the simpler case of critical damping, and the result is

⁵Tomlin, op. cit., p. 435.

⁶Ibid.

$$I_{\text{switch}}(\text{rms}) = I_0 \sqrt{(\text{PRR})L/2R} \left\{ (R^2 C/L + 1) - \exp \left[\frac{-2(\pi - \tan^{-1} \sqrt{4R^2 C/L - 1})}{\sqrt{4R^2 C/L - 1}} \right] \right\}^{1/2}$$

or

$$I_{\text{switch}}(\text{rms}) \approx I_0 \sqrt{(\text{PRR}/2)(RC + L/R)} . \quad (18)$$

The rms current expected through the capacitor is a very important practical consideration. If it is low enough, dc capacitors can be used that are very much less expensive at the voltage ratings needed than their ac counterparts.

Using the results of Eqs. (8) through (18) the following design procedure was carried out. The value of L is 16H and the PRR is 60 pps. From Eq. (6), it was decided to set $t_3 - t_0 = 9\text{ms}$, the maximum allowable response time, according to that criterion. For the design calculations, it was necessary to choose a suitable value of I_0 and design the system to handle this and any smaller value of I_0 it may confront. By substituting 20kV for V_{DC} , 410 for ω and 16 for L into Eq. (3), it can be shown that the largest peak of i_L (i.e. when V_{DC} is largest) is equal to about 3.2 amps. Since the system was designed to clip the top 10% off a 40kV charge waveform, and as shown previously this corresponds to clipping at around $\omega t = 2.5$ radians, the maximum value of $i_L(t_0)$ expected is about $3.2 \sin(2.5) = 3.2(.6) = 1.92$ amps. Therefore, for design purposes, I_0

was set at 2 amps. This is more than enough for practical purposes but it provides a useful set of design figures.

It is obvious from the assumed value of I_0 and L and use of Eq. (16) that the power dissipated in resistor R was expected to be 2080 watts. This value is independent of Q . The design procedure involved programming Eqs. (8) through (18) in an algorithm form into the Hewlett-Packard desk calculator, and feeding in values of Q to obtain proper values of R and C necessary to satisfy the constraints. The algorithm was as follows:

(1) Read in Q

$$(2) \theta = \tan^{-1}(\sqrt{4Q^2-1}) = \omega_0(t_1-t_0)$$

$$(3) \omega_0 = (\pi-\theta)/(9 \times 10^{-3})$$

$$(4) C = (1-1/4Q^2)/\omega_0^2(16)$$

$$(5) R = (\tan \theta)/2\omega_0 C$$

$$(6) \text{ because } I_0 = 2 \text{ amps, } v_{L \text{ max}} = 2R (2\exp(-\theta/\tan\theta)\cos\theta)$$

$$(7) I_{\text{switch}}(\text{AV}) = 60(2)(16(.375 \times 10^{-6}))^{1/2} \\ \times \left\{ \exp(-(\pi-\theta)/\tan \theta) \sin \theta + \sin 2\theta \right\}$$

$$(8) I_{\text{switch}}(\text{rms}) \approx 2\sqrt{30(RC + L/R)}$$

$$(9) I_C(\text{rms}) = I_0 \sqrt{30RC(1-e^{-\pi/\omega_0 RC})} \leq 2\sqrt{30RC}$$

Obviously, for the underdamped case, $Q \geq .5$. Because the dissipation is the important criterion, Q was chosen close to this lower limit. The output for various values of Q are tabulated in Table 1.

Q	C(μ f)	R(k Ω)	v _L max	I _{sw} (AV)	I _{sw} (rms)	I _C (rms)
.55	.119	6.36	9.06kV	.22amp	.63amp	.30amp
.60	.237	4.93	6.80	.28	.73	.37
.625	.300	4.62	6.27	.29	.76	.40
.65	.345	4.43	5.90	.30	.79	.43
.71	.456	4.19	5.40	.30	.83	.48
.80	.612	4.09	5.00	.30	.87	.55
.90	.750	4.15	4.80	.33	.91	.62
1.00	.866	4.29	4.69	.33	.95	.67
1.11	.972	4.50	4.65	.33	.98	.73
1.20	1.050	4.72	4.64	.33	1.00	.78
1.30	1.120	4.92	4.64	.33	1.02	.81
1.40	1.190	5.19	4.65	.32	1.05	.86
1.50	1.230	5.40	4.66	.32	1.07	.89
1.60	1.280	5.65	4.68	.32	1.09	.93

Table I. Design Parameters for De-Q'ing Branch

Based on this table, the proper values of R and C were chosen and this will be discussed in the chapter dealing with the construction of the system. It is noted here that in general as Q increases the necessary value of C increases and so does v_L max and I_C(rms). These data will be used extensively in the later sections of this paper.

2. Theoretical Analysis and Design of the Voltage Divider

Theoretically, it can be shown that the percentage regulation can be affected by the voltage divider used to

sample the network voltage. The following analysis is also given by William Tomlin⁷ of Stanford Linear Accelerator Center. There is a certain fixed delay inherent in the system, mainly through the comparator and trigger circuits. To study the effect of this delay, Fig. 7 is used. The solid line of waveform 1 represents a normal - amplitude PFN voltage. The command to begin regulation is given at point B, and it is assumed that the de-Q'ing signal divider is exactly compensated (zero phase shift) and the system requires about 10 degrees delay, an exaggerated figure for illustrative purposes. Thus, 10 degrees later the regulation process is complete, and the PFN voltage is set at the level represented by C. Next, consider a cycle in which all conditions remain the same but a 25% increase in unregulated PFN voltage occurs as represented by waveform 2. The command to regulate, now B', is given at the same voltage level although occurring earlier in time. The regulated level, again reached after a 10 degree delay, is set at C'. It is readily seen that this latter level represents an increase over the value attained with normal voltage and the accuracy of the regulated waveform suffers.

If the waveform from the de-Q'ing signal divider is now advanced in phase by the required amount, the commands to regulate are given at points A and A' for the normal and increased PFN voltage, and the regulation occurs at

⁷Ibid., pp. 433-435.

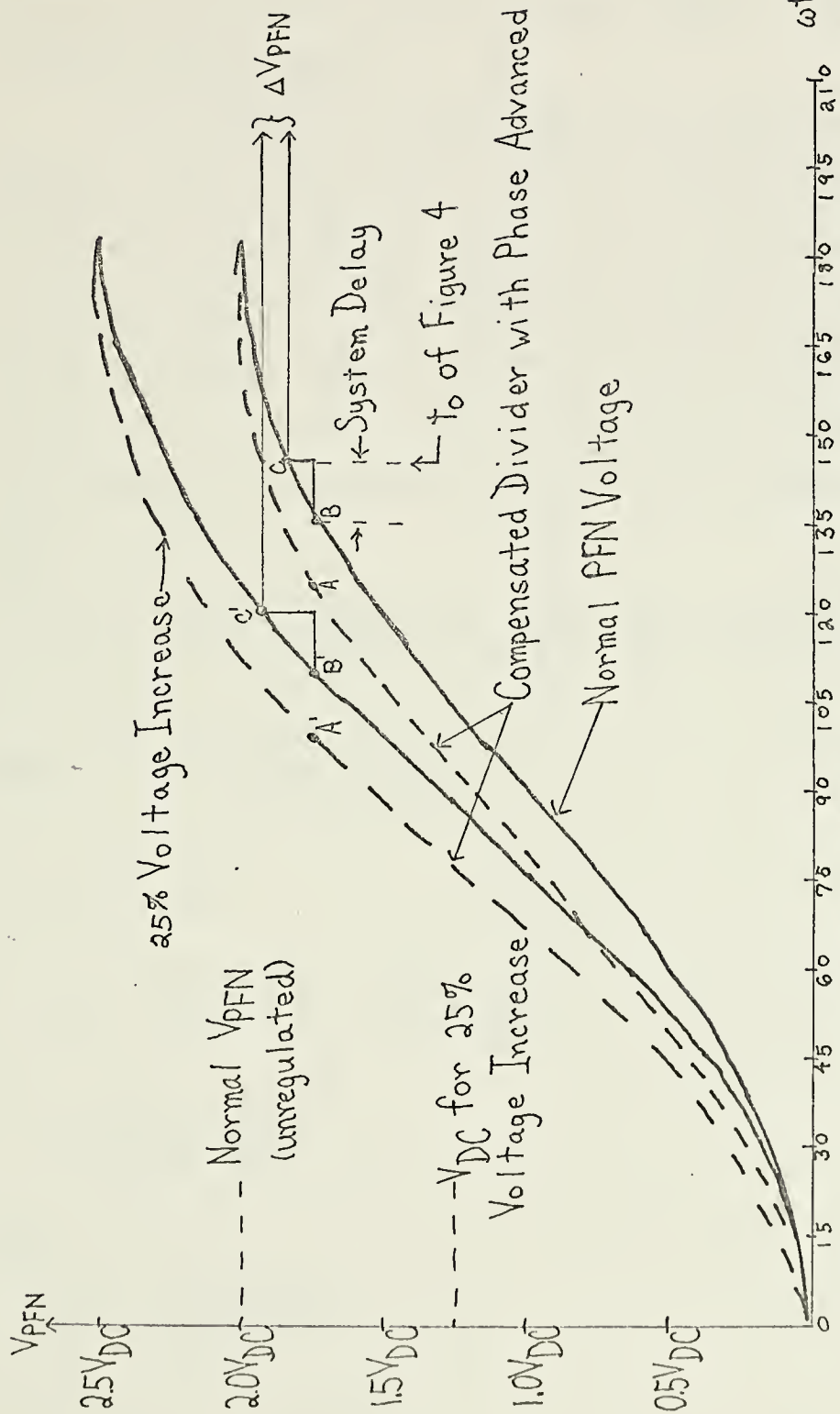


FIGURE 7-COMPENSATED DE-Q'ING SIGNAL DIVIDER
WAVEFORMS

points B and B'. These points now represent the same level of voltage, and the regulation is ideal. It should be noted that if the phase were advanced further the regulated value of the increased voltage would be less than for the normal voltage.

To calculate the phase shift associated with the divider network, consider a divider consisting of n identical sections of R_1 and C_1 and an output section of R_2 and C_2 . This results in $n+2$ simultaneous integral equations. If the voltage divider is driven by the PFN voltage of Eq. (1), the solution for the output voltage across R_2 is represented by the following equation. For $V_{in} = V_{DC}(1-\cos \omega t)$,

$$v_{out} = V_{DC} \times \frac{R_2}{nR_1 + R_2} (1 - K_1 \cos(\omega t + \theta) + K_2 e^{-t/\tau_p}), \quad (19)$$

$$\text{where } \theta = \tan^{-1} \left(\frac{\omega(\tau_1 - \tau_p)}{\omega^2 \tau_1 \tau_p + 1} \right),$$

$$\tau_1 = R_1 C_1,$$

$$\tau_p = \frac{nR_1 R_2}{nR_1 + R_2} \left(\frac{C_1}{n} + C_2 \right) \approx R_2 C_2,$$

$$K_1 = \left(\frac{\omega^2 \tau_1^2 + 1}{\omega^2 \tau_p^2 + 1} \right)^{1/2}$$

and

$$K_2 = \frac{\omega^2 \tau_p (\tau_1 - \tau_p)}{\omega^2 \tau_p^2 + 1}.$$

Note that Eq. (19) reduces to the input waveform reduced by the resistive ratio when $\tau_1 = \tau_p$. To compensate for the additional circuit delay in firing the thyatron τ_1 and τ_p should be chosen such that θ exactly equals the system delay. The phase shift should be constant, and this requires that the last term in Eq. (19) go to zero before the earliest reference to the waveform. As discussed in the first part of this chapter, the earliest reference to this waveform (command time) is around 6 ms. Therefore τ_p should be chosen such that $5\tau_p \leq 6 \times 10^{-3}$, allowing five time constants for complete decay. Also, in calculating R_2 and C_2 , consideration must be given to the input resistance and capacitance of the comparator circuit, and any cable capacitance between the divider and comparator. The choice of R_1 in high voltage circuits must take into consideration power dissipation and voltage rating and the desired time constant. The number of sections required is then determined. The resistors should also be noninductive with low temperature coefficients and low thermal noise. A further consideration is corona, which is associated with circuits operating above 30kV. For this reason, it is desirable to immerse the divider in oil. As the system time delay is never known exactly when the original system is installed, the practical approach is to calculate R_1 , R_2 and C_1 and then adjust C_2 for best regulation when the system is in operation.

The conditions of Eq. (19) were used and a compensated divider was initially used in the system. This will be discussed later in the paper.

B. EMPIRICAL DESIGN

The two major components which were designed empirically are the comparator and the trigger circuit.

1. The Comparator Circuit

Figure 8 shows the circuit diagram of the comparator. This module compares the sampled PFN voltage to a variable dc reference voltage and provides an output signal whenever the PFN sample exceeds the reference. Because of the low cost, ease of replacement, and high input impedance of the Fairchild $\mu 709$ and $\mu 741$ operational amplifiers (op-amps), it was decided to use either of these as the main element in the comparator.

The open loop gain of either of these op-amps is on the order of 15,000. Thus, because the inputs are subtracted, and the difference amplified, a small (1mV) differential voltage between the inputs is enough to drive the output into saturation at either -15 volts, or +15 volts. The op-amp used in this way, then, is really an amplitude controlled switch. If the reference voltage is set at a certain value, then the op-amp output will hold at -15 volts until the sampled PFN voltage rises to about 1mV above the reference and then will hold at 15 volts.

The emitter-follower is used to provide enough output current to break down the gate of the triac in the

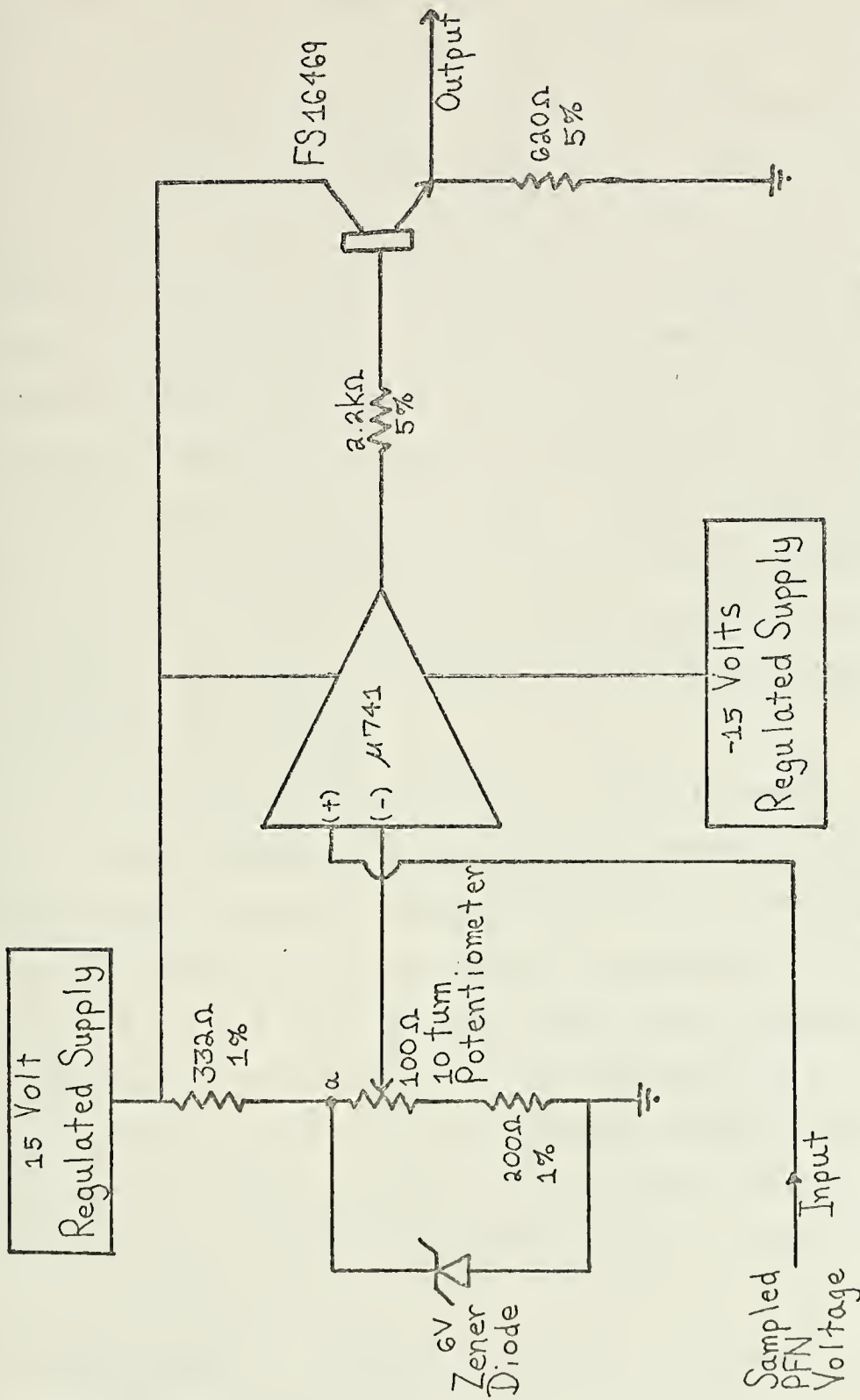


FIGURE 8 - FINAL CIRCUIT DIAGRAM OF THE COMPARATOR CIRCUIT

input stage of the trigger chassis. They are described in the next section of this paper. The maximum output current of the op-amp is only 10ma, and the triac used requires close to 25ma on its gate. The emitter follower acts like a current amplifier and provides enough current to initiate the trigger pulse. When the op-amp output is low, the base-emitter junction of the transistor is reverse-biased, and there is no voltage out. When the op-amp goes high, about 7ma are drawn by the base of the transistor. This is enough to drive the transistor into saturation, and the output voltage rises to 15 volts. Obviously one requirement on the transistor is that its collector current can exceed 25ma. Without connecting the output to the trigger chassis, the output voltage is 15 volts across 620Ω which is the required 25ma.

The reference voltage is varied by means of a ten-turn potentiometer, and the resistor string is designed such that this reference voltage can be varied from four to six volts. Without the zener diode, the voltage at node "a" would rise to 7.1 volts. The zener diode, however, breaks down when v_a reaches 6 volts, and begins to draw current. If v_a is held at 6 volts, the current through the 332Ω resistor is $9/332 = 27\text{ma}$, and the current through the potentiometer and the 200Ω resistor is $6/300 = 20\text{ma}$, leaving 7ma to be conducted through the zener diode. As the arm of the potentiometer is shifted, the range of voltage covered is from 4 to 6 volts.

The non-inverting input of the op-amp is obtained from the voltage divider which attenuates the PFN voltage by a suitable factor. The total resistance of the divider string is about 40 megohms. It consists of seventy-two 560k Ω carbon resistors in series. Because the largest V_{PFN} expected is 40kV, and the reference level for de-Q'ing should be lower than this anyway, the output resistor in the voltage divider was chosen to be 6.3k Ω . This would cause 38kV to appear as 6V at the op-amp input terminal. The maximum input voltage that the op-amp can handle is ten volts. With a 6.3k Ω carbon resistor as the output resistor, the theoretical range of de-Q'ing is from 25.4kV to 38kV. By making this output resistor carbon, temperature stability is achieved, because all resistors in the string have the same temperature coefficient.

2. The Trigger Chassis

The purpose of the trigger chassis is to fire the de-Q'ing thyatron.

a. Description of a Thyatron⁸

A thyatron is a gas-filled tube (in this case hydrogen) which consists of essentially an anode, a control grid, and a cathode. The cathode is the source of electron emission. With a positive voltage on the anode, the tube will remain in a non-conducting state if a suitable voltage

⁸Hydrogen Thyratrons, English Electric Valve Co. Ltd., England, Jun 1964, p. 3.

(usually negative but zero is sufficient) is applied to the grid. This voltage depends on the anode voltage and for every value of anode voltage there is a critical grid potential.

The electrons leaving the cathode are prevented from reaching the grid/anode space by the potential barrier at the grid. As the grid voltage is made less negative, or the anode voltage more positive, the field due to the anode attracts an increasing number of electrons from the cathode. These make collisions with gas atoms, and when the electrons produced are accelerated to the ionization potential of hydrogen and sufficient collisions occur, cumulative ionization takes place and the tube fires through. The voltage across the tube then drops to a low value. The current passed is then largely determined by external circuitry.

During breakdown the negative potential on the grid attracts positive ions and these form a sheath through which the grid potential cannot penetrate. Thus, any increase in the negative value of grid supply voltage has no effect on the current passing. The tube will return to its non-conducting state only after removal of the anode voltage for a sufficient time (called the recovery time) to allow the charged particles to be swept away or neutralized by recombination. The voltage on the grid then returns to its original value, and a positive voltage can be reapplied to the anode without conduction taking place. The tube therefore acts as an electronic switch which may be closed by

the application of a positive signal to the grid, but which can only be opened by the removal of anode voltage for minimum time.

b. Trigger Circuit Requirements

It was required that the trigger signal applied to the thyatron grid be from a low-impedance source, have a high rate of rise of voltage and a pulse amplitude sufficient to cause rapid ionization of the gas in the grid-cathode space. This minimizes jitter and anode delay time drift. The required pulse amplitude and duration is specified by the manufacturer of the tube. For this application, the thyatron had to be capable of withstanding approximately twenty kV anode voltage, and handle around half an ampere average current. The Tung-Sol Industrial electron tube type 5948A is rated at 25kV maximum forward and reverse anode voltage. It is also rated at one ampere average current. There was a large surplus stock of these tubes available, so this particular tube was chosen as the de-Q'ing thyatron.

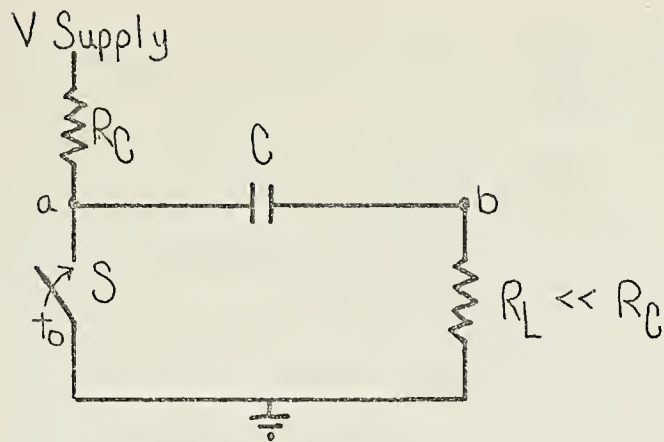
According to specifications the 5948A requires a trigger pulse having a maximum risetime of $0.35\mu\text{s}$, and a pulse width of $2\mu\text{s}$ at 70.7% of peak. The grid pulse peak is specified between 700 and 1800 volts, and the grid impedance varies with the voltage applied. For a peak voltage of 1500 volts, the grid impedance is 200Ω . Thus, the energy required to turn the thyatron on is seen to be the

peak power multiplied by the pulse duration, or $(1500)^2(2 \times 10^{-6})/200$ and this is equal to .0225 joules.

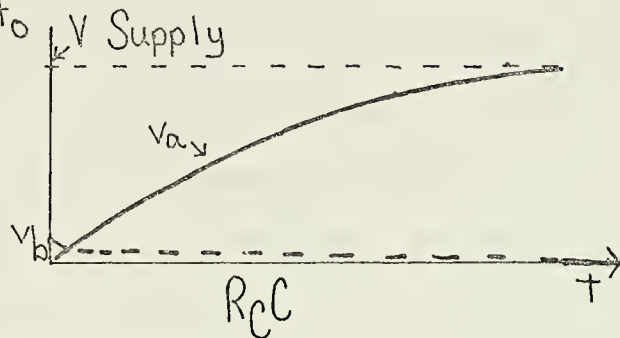
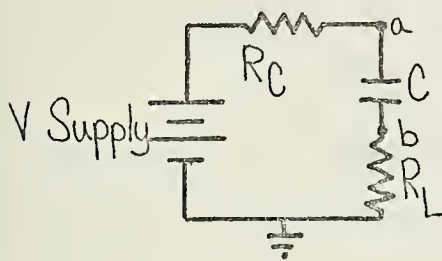
c. General Principle Behind the Trigger Circuit

It was decided that to provide a pulse having the specified rise-time and close to the proper duration, the simplest method would be as follows. Figure 9 shows a simple diagram of the basic idea. From time $t=0$ to t_f , switch S is open and the capacitor charges toward voltage V_{supply} . At $t=t_f$, switch S closes, and suddenly the charged capacitor is forced to discharge through the low impedance load. But at $t=t_f$, because the high-voltage side of C becomes grounded, the voltage across the load has to fall to $-V_{\text{sup}}$ instantaneously. C discharges through R_L so the voltage across the load is very soon back to zero and the current ceases. Because $R_L \ll R_C$, the time constant is very short. Once the current ceases, the switch S opens again and the cycle repeats.

Note that this type of arrangement produces a very sharp negative spike across the load resistance. In order to invert this spike, and also to increase the peak voltage produced, one merely has to replace R_L with a pulse transformer having a suitable turns ratio and the proper polarity. Of course, this introduces a reactive component into the circuit (the leakage inductance of the transformer) but in general if the impedance of the transformer is kept low enough, a fast rising pulse can be generated using this method.



Equivalent Circuit Before t_0



Equivalent Circuit After t_0

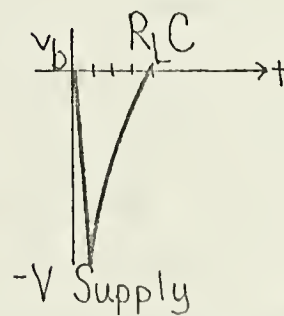
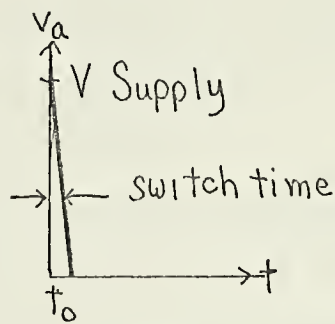
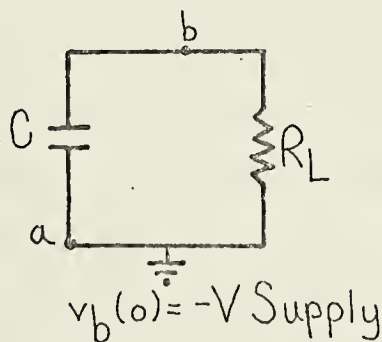


FIGURE 9-PRINCIPLE BEHIND TRIGGER CIRCUIT

There are two possibilities for switch S. One is a small thyatron, and the other is a solid-state version like a silicon controlled rectifier (SCR). Both are functionally alike in that they remain open until triggered by a suitable positive pulse and then remain in a conducting state until the current across the switch either reverses direction or remains at zero for a minimum time. A version of the SCR, called a triac, was used for one stage of the trigger circuit. It acts like an SCR but it can be triggered by either a positive or negative pulse.

At higher voltages, it seems as though small thyatrons are cheaper than SCR's. Also, the turn-on time (which actually determines the rise-time of the generated pulse) of a thyatron is much faster than that of an SCR. Therefore, for the output stage of the trigger chassis, a small thyatron, the 3C45, was used as the switch.

d. Operation of the Trigger Circuit

Figure 10 shows the final circuit diagram of the trigger chassis along with the isolation pulse transformer. The circuit uses two stages of capacitor-discharge-generated pulses, the output pulse being fed into the grid of the de-Q'ing thyatron. The output pulse transformer serves to both invert the generated spike, and insulate the trigger circuit from the grid of the de-Q'ing thyatron. Since the plate voltage of the de-Q'ing thyatron approaches 40kV, this was the amount of voltage insulation required.

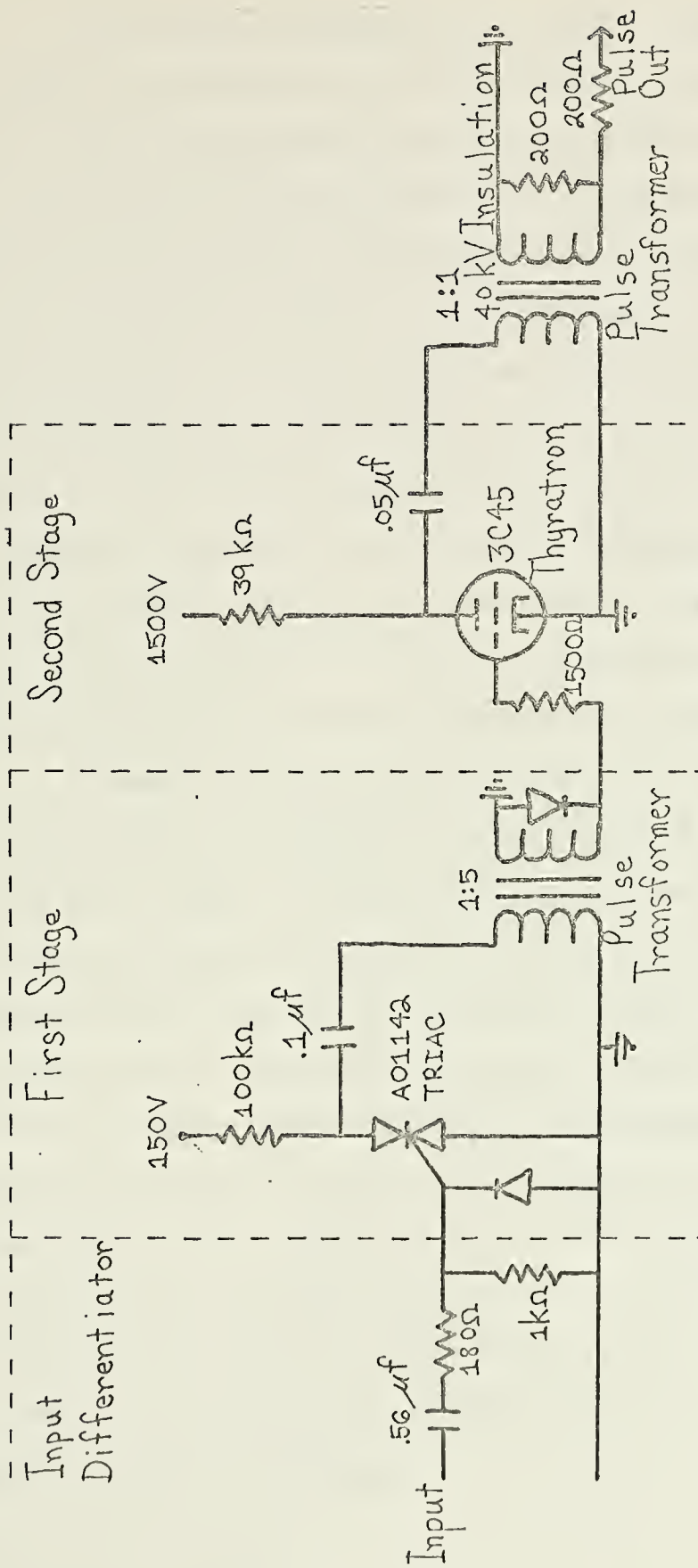


FIGURE 10-CIRCUIT DIAGRAM OF TRIGGER CHASSIS
AND OUTPUT PULSE TRANSFORMER

The circuit operates as follows. The input signal will only assume one of two possible states, 0 or 15 volts, with a switching time of about 100 μ s between states. When the input is 0, there is no signal applied to the gate of the triac, and therefore the triac does not conduct, and the .1 μ f capacitor must charge to 150V through the 100k Ω resistor. During this time, the voltage across the first stage pulse transformer is 0, so there is no signal applied to the grid of the 3C45 thyatron. This thyatron therefore does not conduct and the voltage at its plate rises exponentially toward 1500 volts with a time constant $(39)(.05)(10^{-3}) = 1.95\text{ms}$. The voltage across the output transformer is zero and there is no output.

When the input signal switches to 15 volts, the gate of the triac is initially pulled high and the gate will draw about 25ma. The input signal at the gate, however, will then decay exponentially with a time constant determined by the .56 μ f capacitor and the gate impedance in the on condition. This spike is enough, however, to cause the triac to conduct, and the first stage exhibits the kind of action discussed previously and produces a negative voltage spike at the primary of the pulse transformer of around 90 volts. The pulse transformer is a 5:1 step up and the pulse at the grid of the 3C45 is about 450 volts high. This is well above the minimum value of 175 volts required to turn the 3C45 on.

Due to some leakage inductance in the pulse transformer, some of the energy initially stored in the capacitor will temporarily be stored in this inductance, and once the capacitor is discharged, the current will try to reverse direction as the inductance and capacitor exchange energy. This is known as "ringing", and a small amount of it is useful for insuring that the triac is turned off. But if the reverse swing is too large, the triac may break down, so to increase the damping of the reverse signal, a diode is placed on the secondary of the first pulse transformer.

When the 3C45 conducts, the .05 μ f capacitor (which is fully charged in about 10ms, and contains .056 joules) discharges through the low impedance path of the forward conducting resistance of the 3C45 and the equivalent impedance of the pulse transformer. A 1500 volt spike is generated and fed to the grid of the de-Q'ing thyratron. Again the leakage inductance of the pulse transformer causes ringing, but the reverse swing is not as severe on the 3C45 and no reverse-damping diode is necessary here. The ringing insures that the 3C45 is turned off and the whole cycle repeats.

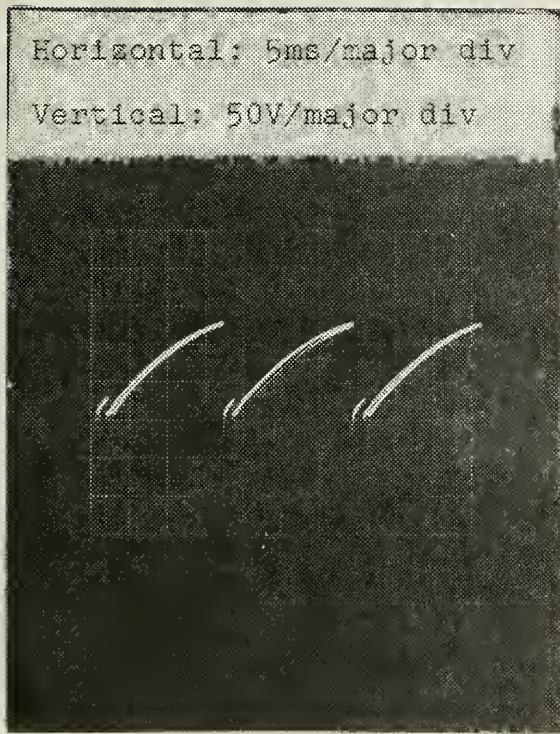
Because the generated pulse is ultimately caused by the arrival of the sampled PFN voltage at the reference level, and this can occur at most sixty times per second, the trigger pulse must be produced at a repetition rate of

60pps. This allows 16.7ms for the capacitors to recharge between cycles.

Finally, the purpose of the diode in the input differentiator will be discussed. The triac, as mentioned earlier, will conduct when either a positive or a negative pulse is applied to its gate. When the input signal is switching from 0 to 15V, the positive pulse is generated, but when the input signal drops from 15 to 0, a -15 volt spike could appear at the gate of the triac, were it not for the diode. Since it was desired only to fire the triac (and generate the output pulse) on positive transients of the input, the diode was essential.

Figures 11(a) and 11(b) show the anode voltage waveforms recorded for the triac and 3C45 respectively. Figures 12(a) and 12(b) show the open circuit pulses to be applied to the grids of the 3C45 and 5948 thyratrons respectively. The latter is the trigger chassis output.

Figure 13 shows the grid pulse applied to the grid of the 5948 thyatron in two views. The first is an overview and shows the entire effect of the pulse on the thyatron. The second view is the beginning of the pulse, expanded in time. Note the similarity between this view and the view of the open-circuit pulse of Fig. 12(b).



(a) Voltage at anode of
triac AO1142

(b) Voltage at anode of
3C45 thyatron

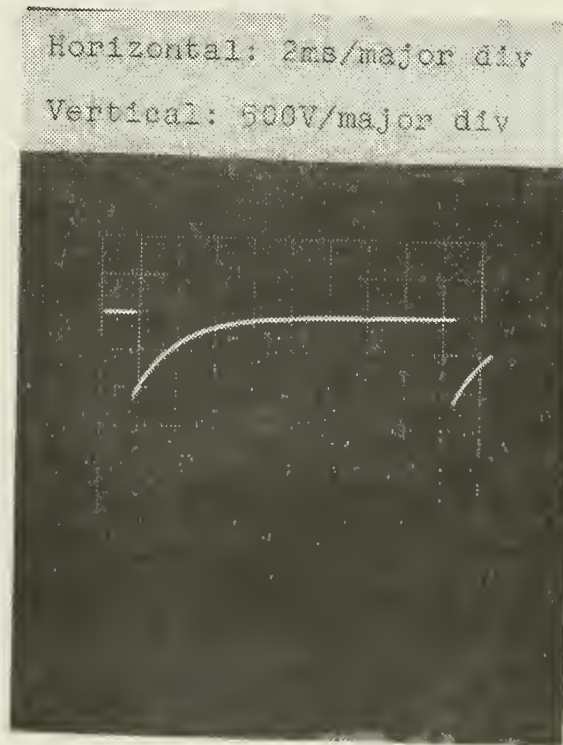
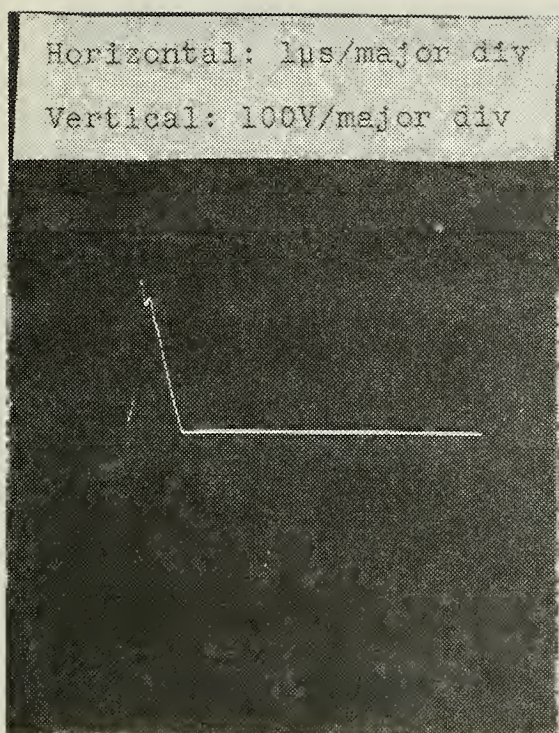


Figure 11. Anode Voltage Waveforms in the Trigger Chassis



(a) Output of stage 1 of trigger chassis

(b) Output of stage 2 of trigger chassis

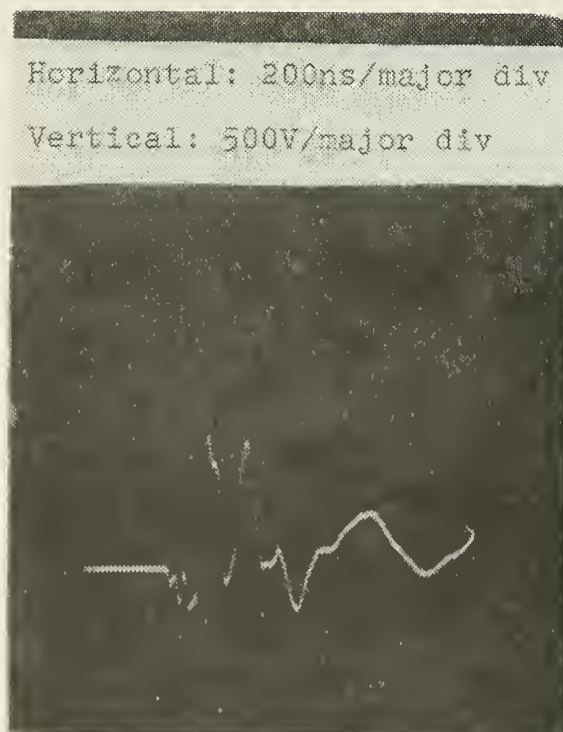
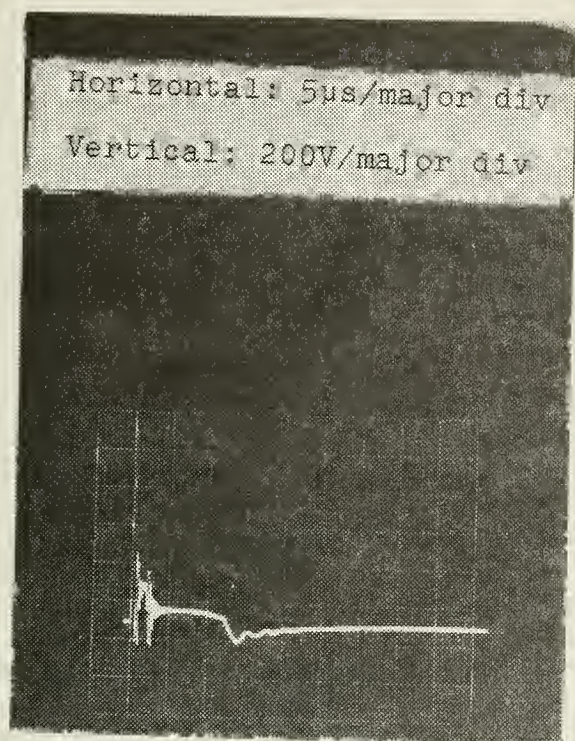


Figure 12. Open Circuit Generated Pulses



(a) Full waveform showing initial turn-on, voltage plateau and grid recovery

(b) Expanded time view of pulse showing initial breakdown of grid

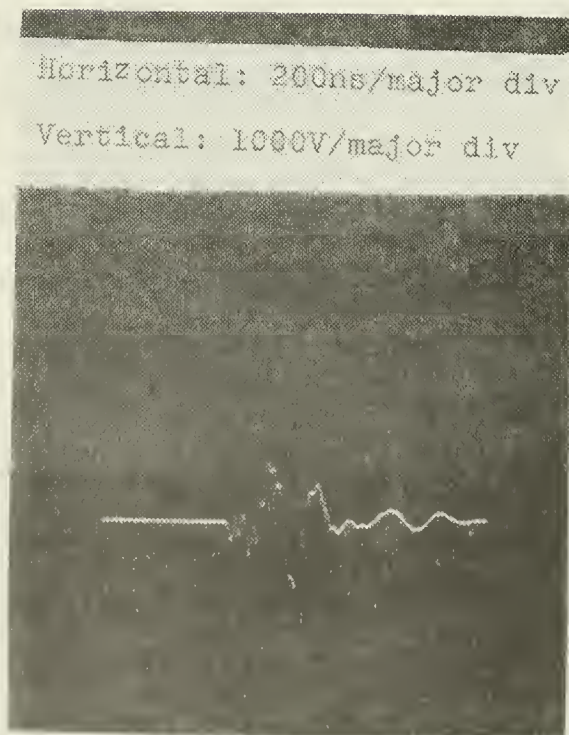


Figure 13. Grid Pulse Triggering de-Q'ing Thyatron

III. CONSTRUCTION OF THE PROTOTYPE

The system was constructed as a prototype, servicing one of the three modulators. In this section the details of that construction will be discussed.

A. CONSTRUCTION OF THE DE-Q'ING BRANCH

The first step in constructing the de-Q'ing branch was to choose suitable values for R and C . Based on the data of Table I in the previous chapter it can be seen that a desirable value of R was in the range of from four to five $k\Omega$, while C had to be between 0.2 and 1.1 μf . There was a surplus stock of dc filter capacitors having 16kV insulation and rated at 0.5 μf . Two of these were chosen, and the value of C could be changed during testing to three different values.

The value of R was chosen to be 5 $k\Omega$, placing the value of Q at .625 for $C = .5 \mu f$. This value of R caused the frequency ω_0 to be slightly higher than that indicated in the table, and theoretically should cause the current in L to die out within 8.33 ms, which is lower than the 9 ms used for the design calculations.

As seen in the previous chapter, the power expected to be dissipated in R was about 2kW. In order to keep the resistors from getting too hot, it was decided to rate the total resistor bank at 5kW. This required that twenty-five

200W resistors be used. Each resistor is wire-wound and rated at $5k\Omega$. The bank is arranged in a five-by-five series-series-parallel matrix, and mounted on a wooden plank about 6 feet by 1 foot.

The next part of the de-Q'ing branch to be constructed was the hold-off diode, whose purpose it is to keep the branch from conducting current after the PFN discharges when the total voltage across the branch becomes negative. There was also the possibility of very large negative voltage spikes generated when the PFN discharges coupling back to the de-Q'ing network, so the diode bank was designed to handle 50kV inverse. Fifty avalanche diodes rated at two amperes forward current and 1kV PIV were connected in series. However, because each diode conceivably has a slightly different leakage current, a string of reversed-biased diodes can be thought of as a string of slightly different resistors. As in any resistor string the highest resistance (in this case the best diode) would take the largest portion of the total voltage across the string. Thus, if the total inverse voltage should ever approach 50kV, it would be quite possible to have more than the rated PIV across one diode in the string, thereby breaking down the diode and burning out the string. To eliminate this problem in advance, the string is "balanced" by shunting each diode by an equal resistance much lower than its equivalent reverse-bias resistance. This, along with equal shunt capacitors much greater than the equivalent capacities

of the diodes, maintains equal voltages across each diode in spite of individual diode differences. The values chosen, and the arrangement are shown in Fig. 14(a). The resistors, of course, conduct current when the diode is off, but the relative time constant is long enough to preserve the unidirectional nature of the string.

The next piece of circuitry to be constructed for implementation of the de-Q'ing branch was the heater/reservoir power supply. The heater current required by the Tung-Sol 5948 thyatron is between 25 and 33 amperes. This thyatron also requires current to what is known as a "reservoir" within the tube that keeps the pressure of the hydrogen gas constant. The current required by the reservoir is 3 amperes. The filament (heater) voltage is rated at 6.3 volts and the reservoir voltage is 4.1 volts.

The filament transformer required must thus be capable of supplying at least 6.3 volts rms at 28 amperes. The voltage insulation required between the primary and secondary of the transformer is forty kV. There were available three filament transformers, each rated at .75kVA, 110/10, 75 amperes secondary current. These transformers are fairly large (8"x8"x11") and it was desirable to use one per thyatron. In order to supply both the heater and reservoir with the same filament transformer, the arrangement shown in Fig. 14(b) was used.

This circuitry was placed on a small moveable cart along with the trigger output pulse transformer, and wheeled into

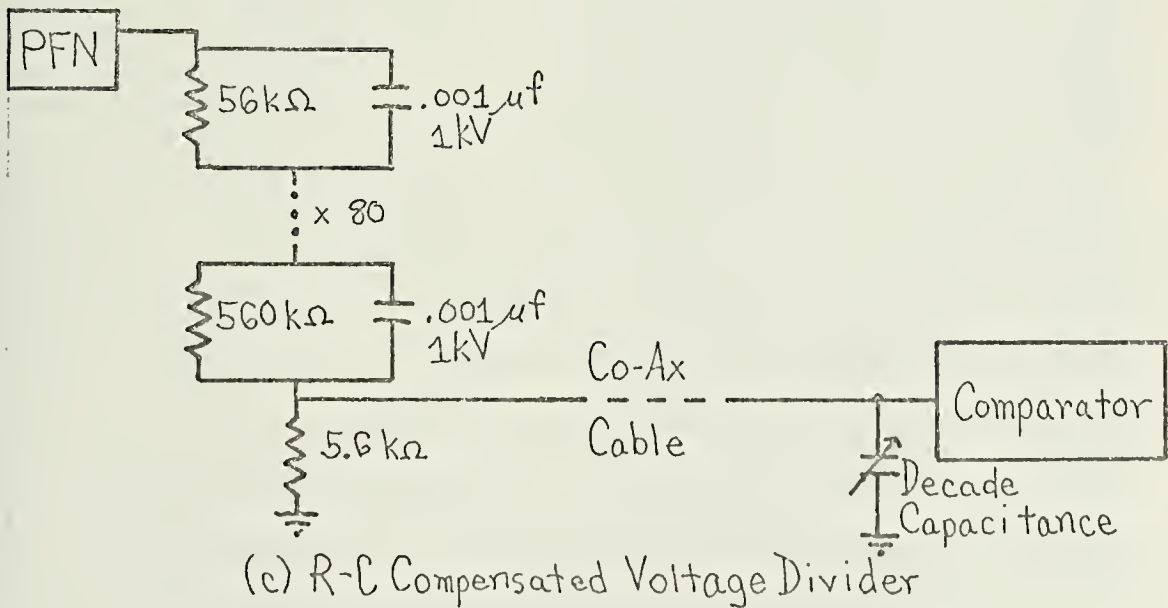
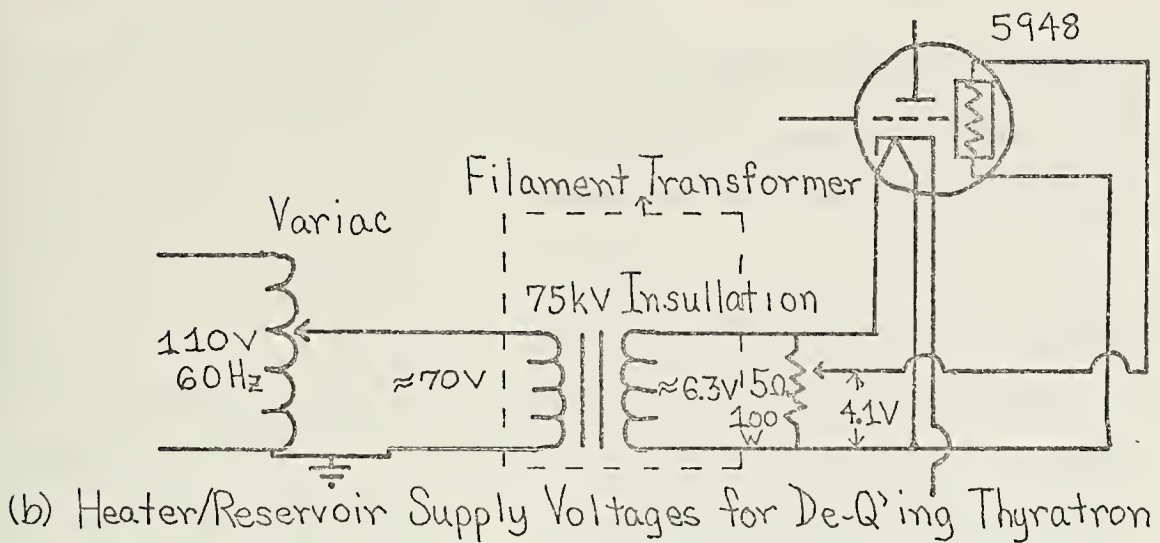
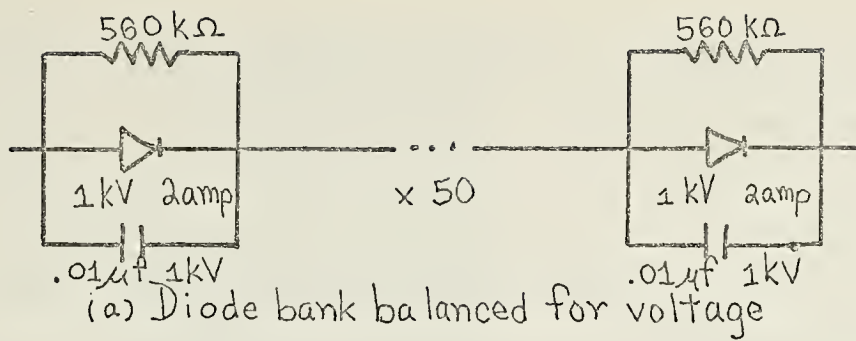


FIGURE 14-MISCELLANEOUS
CIRCUITRY CONSTRUCTED

the high voltage cage for temporary installation and testing. Figure 15 shows the actual physical arrangement of the elements.

B. CONSTRUCTION OF PULSE TRANSFORMERS

There were two pulse transformers as shown in Fig. 9. The step-up transformer connecting stages 1 and 2 was wound on a ferrite toroidal core using thin copper wire. There are five turns on the primary and twenty-five on the secondary. The voltage insulation required, only fifteen hundred volts, was not critical.

The output pulse transformer, however, was required to have forty kV voltage insulation. There were available some 3mH chokes with 0.3 resistance which consisted of a large core of laminated iron with two legs. Each leg was close-wound with fifty turns of copper wire and the coils were connected in series by a shorting bar. By disconnecting the shorting bars, the chokes made suitable 1:1 pulse transformers. Because the spacing between the core and the windings and between the separate windings was only 0.25 inches, there would not be enough insulation if the transformer were used in air. However, immersed in an oil bath the quarter-inch spacings provided more than enough insulation. A pyrex jar was used and a suitable container was fashioned. The transformer in the jar can be seen in Fig. 15.

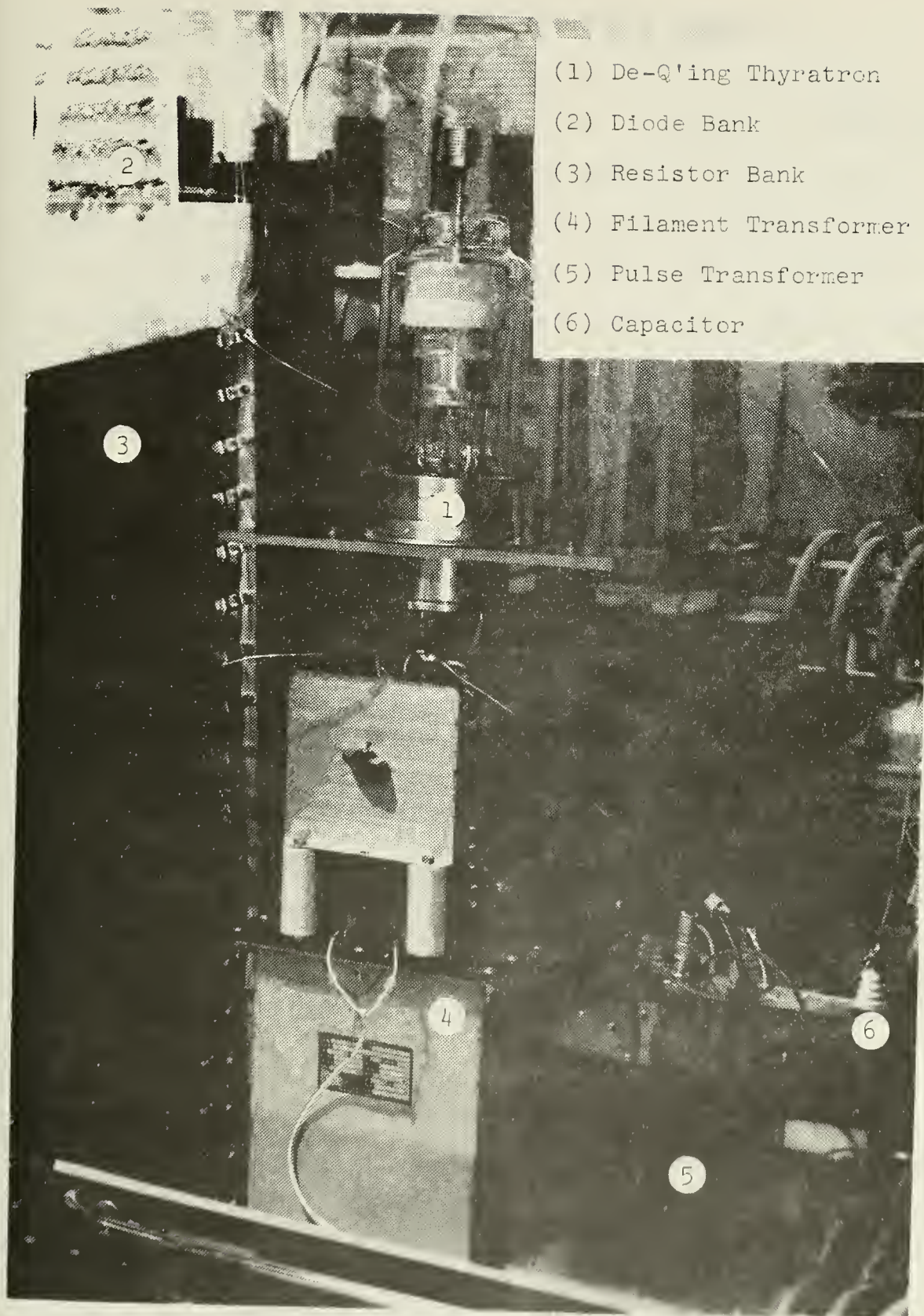


Figure 15. Physical Layout of De-Q'ing Branch.

C. CONSTRUCTION OF THE REMAINDER OF THE PROTOTYPE

The remaining parts of the system were constructed, the trigger chassis according to Fig. 10, and the comparator as in Fig. 8. The trigger chassis was built into a rack mount with enough room for two more similar modules in the future. It was placed in a mobile rack stand along with the two auxiliary dc supplies and placed just outside the high voltage cage.

The comparator was mounted on a small circuit board, and will eventually be fabricated in a printed circuit. The ten-turn potentiometer, a Helipot, is the largest element in this circuit and its dial is adjusted by the operator. This module is in the control room. Figure 16 shows roughly the location of each part of the prototype. The electrical connections are made using coaxial cables.

D. CONSTRUCTION OF THE R-C COMPENSATED VOLTAGE DIVIDER

Because the original design called for the compensated voltage divider (see Fig. 5), this was constructed using the conditions derived with Eq. (19). The value of R_1 was chosen as 560k Ω mainly because these resistors were available in large quantity. For the same reason, C_1 was chosen as .001 μ f, 1kV. To make the string a total of slightly over 40M Ω , it was made eighty sections long. The resistor R_2 was chosen as 5.6k Ω , giving a resistive ratio of 1:8000. This string was mounted in a pyrex box which was then filled with insulating oil to avoid any high voltage

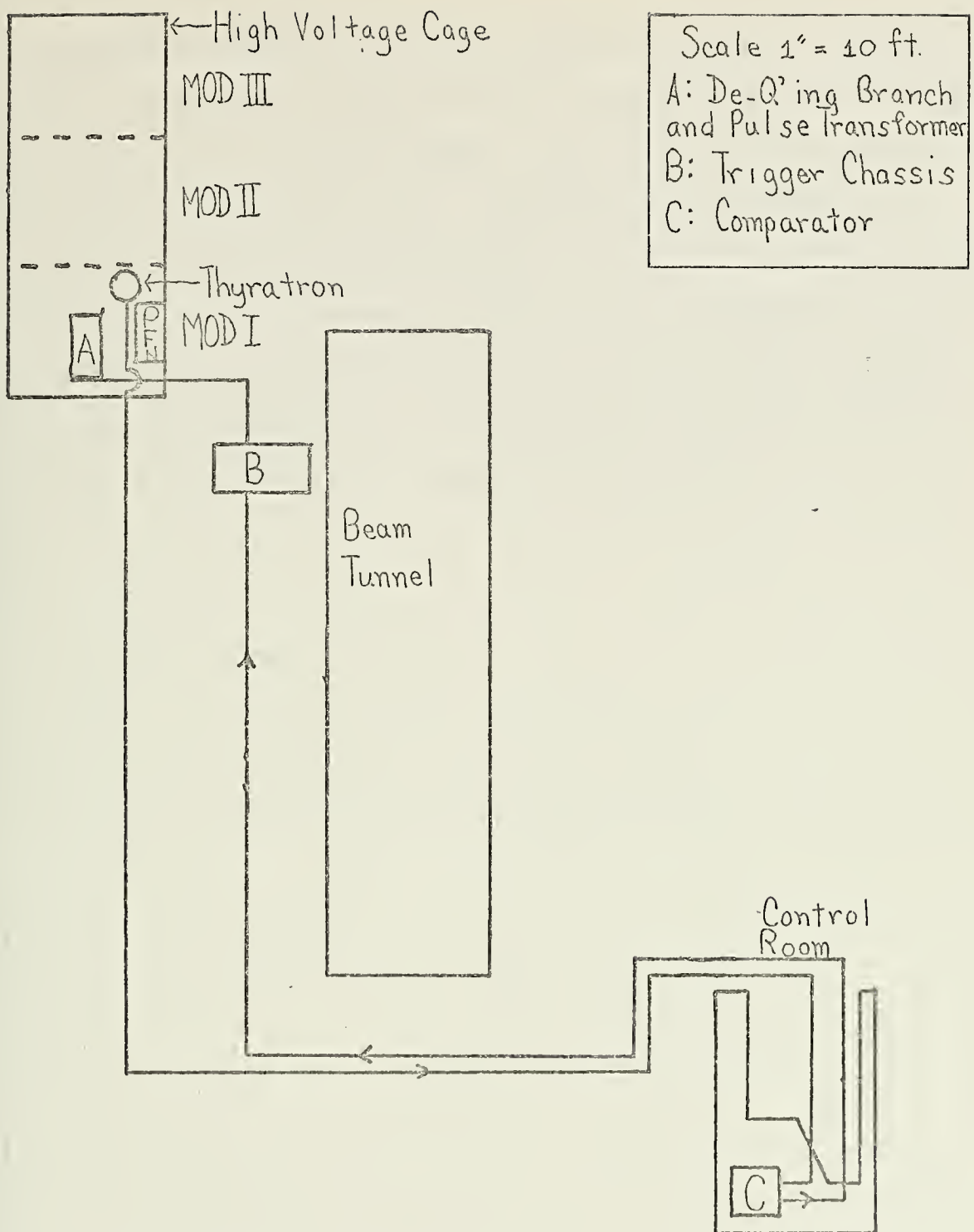


FIGURE 16-ROUGH SKETCH OF APPROXIMATE PHYSICAL LAYOUT OF PROTOTYPE SYSTEM

transient effects across the capacitors, such as corona. The string was initially set up (as shown in Fig. 5) at the anode of the charging diodes. Thus, this string was located in the high voltage cage. A coaxial cable connected R_2 to the comparator circuit where a variable capacitance was shunted across the input terminal of the comparator. By varying this capacitance (C_2) the relative phase between the output and input of the compensated divider could be varied. Figure 14(c) shows the arrangement.

IV. TESTING OF THE PROTOTYPE

A. TESTS PRIOR TO PROTOTYPE INSTALLATION

In order to obtain a quantitative measure of the effect of the de-Q'ing circuit on the system, the voltage regulation was measured prior to installation of the prototype. Without de-Q'ing it was generally known that the variation in pulse amplitude was directly related to fluctuations in V_{DC} . The system includes two monitors for V_{DC} . One is a milliammeter which measures average dc voltage into the system and is calibrated for 25kV full scale deflection. This is used in setting the coarse value of V_{DC} and is usually fixed at .72 or 18kV. The second monitor is a finer measure of V_{DC} fluctuations. It is a balanced bridge arrangement as shown in Fig. 17. After a suitable V_{DC} is set by the operator, the switch is closed, and the potentiometer dialed in until the meter reads null. Then any deviation from the initial value of V_{DC} will be indicated by the deflection of this meter movement. During operation, it is desirable to maintain the meter movement within the sectors marked green. One of the biggest problems to the system without de-Q'ing was the sudden application of another load on the ac lines in the building. The one having the most noticeable effect on the system was a pump which would suddenly switch on at various times during a LINAC experiment, and create a transient drop in overall line voltage which could be seen at the LINAC in complete

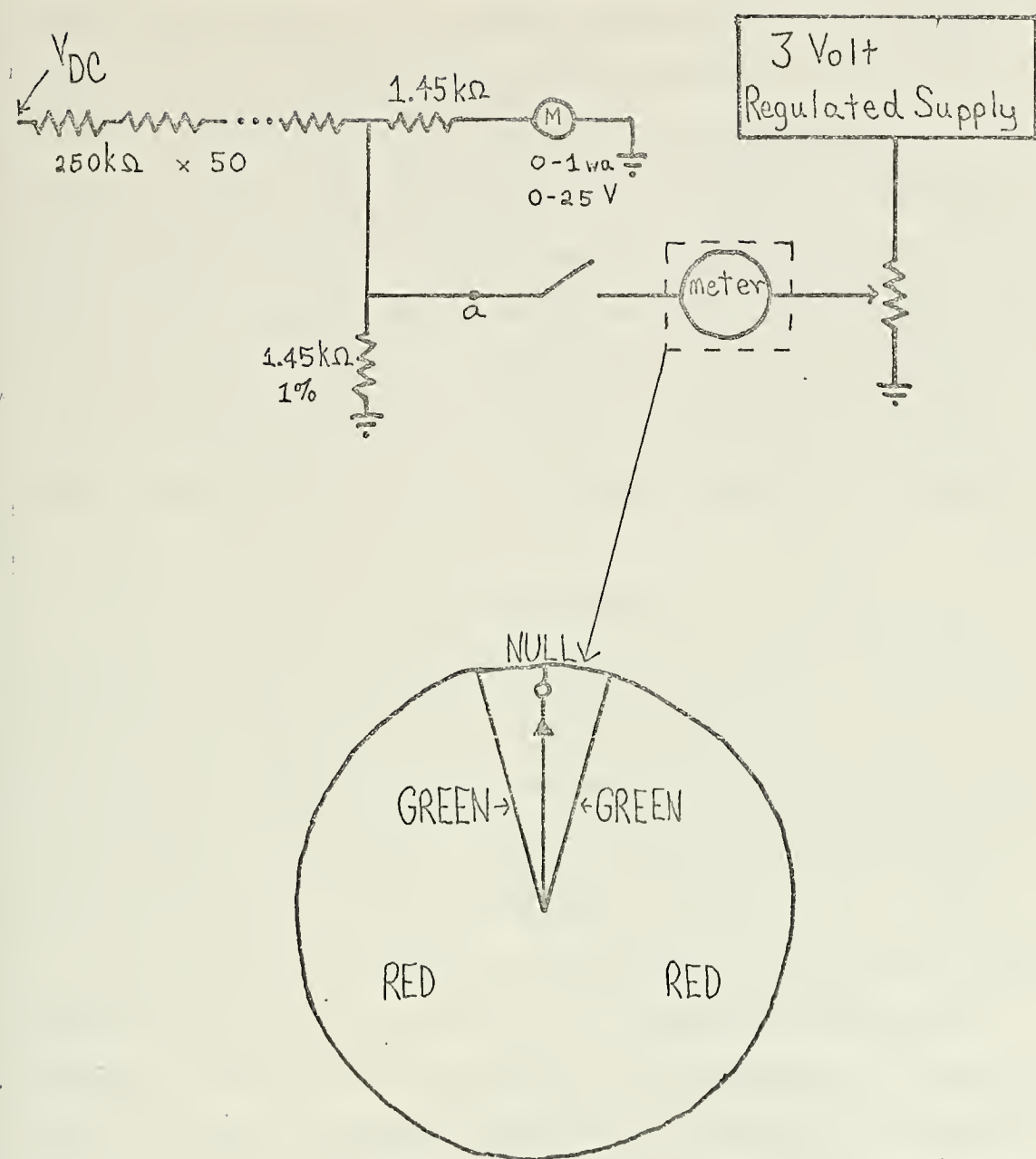
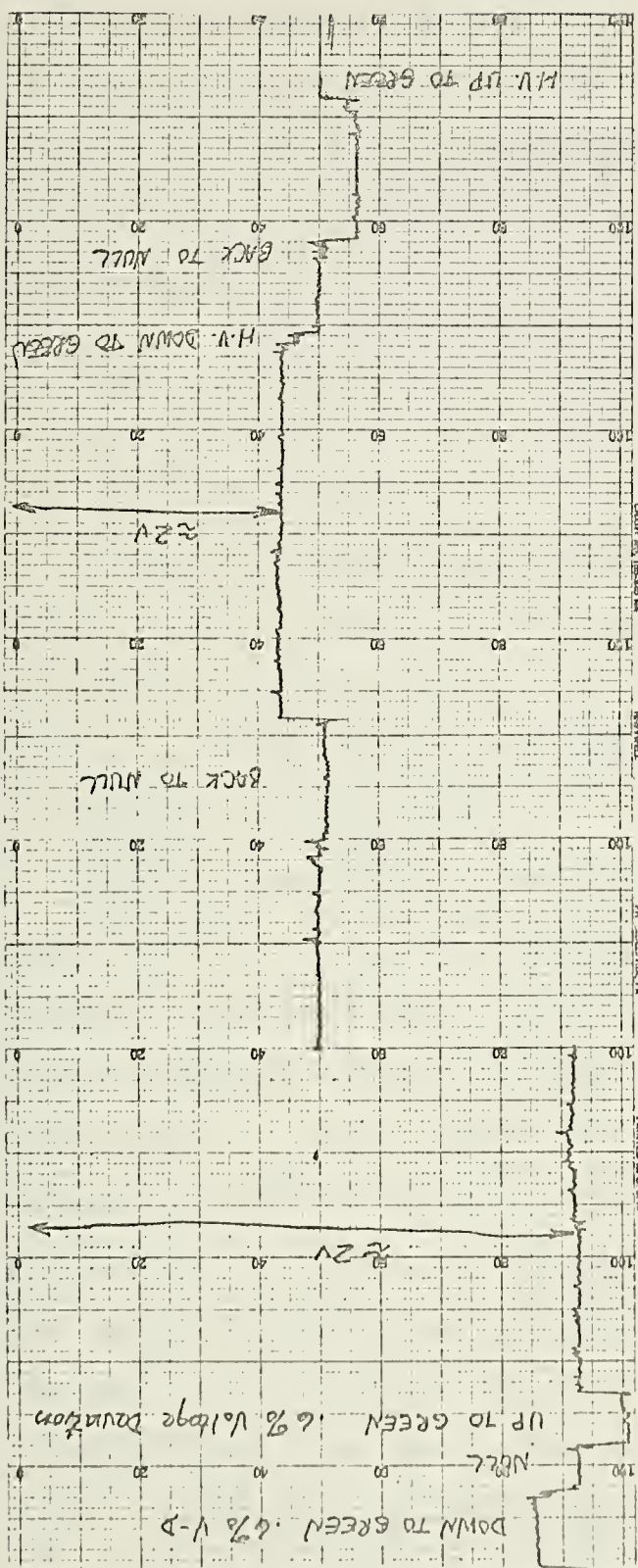


FIGURE 17-PRESENT HIGH VOLTAGE MONITORS AT CONTROL PANEL

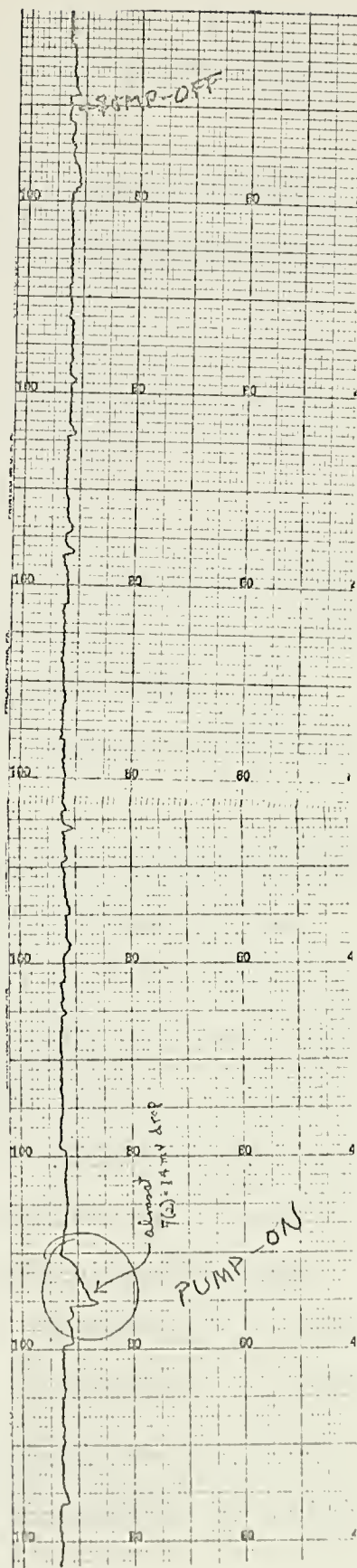
loss of electron beam. Correlated with this loss of beam was always a shift of the meter movement in the bridge circuit from the green into the red region. The usual process, without de-Q'ing, was for the operator to try to keep the meter movement in the green region by operating a servo motor through buttons on the control panel. The servo motor controls the setting of the variac that controls the amount of ac voltage that enters the power supply. During machine operation the meter movement would also stray slightly from null over periods ranging from minutes to hours.

The first test before installation of de-Q'ing was to actually measure the percentage of fluctuation corresponding to the bridge circuit meter movement moving from null to the red region. A strip recorder was connected at point a (see Fig. 17), and the input voltage and potentiometer were adjusted until the meter was null for $v_a = 2$ volts.

The 2 volt line was then centered on the strip recorder printout and the sensitivity was changed to 20mV/major division. The input voltage was then increased to the point where the meter movement just passed from green to red on the right and held there. Then the voltage was decreased so the meter was again nulled. Then the voltage was decreased until the meter movement crossed to the left into the red. The strip chart recording is shown in Fig. 18(a).



(a) Controlled



(b) Uncontrolled

18. Chart Recordings of Typical Variations in V_{DC}

The uncontrollable surge caused by the pump was also measured under the above conditions, and the pump turn-on and turn-off is indicated in Fig. 18(b).

From the figure, the percentage of fluctuation necessary to cause a movement from null to the green-red boundary is calculated below

$$\% \text{ dev.} = \Delta v / V_{\text{null}} \times 100\% = (12 \times 10^{-3} / 2) \times 100 = .6\%$$

$$\% \text{ dev} |_{\text{pump surge}} = .7\%$$

This test showed three things: (1) the maximum expected short term variation in V_{DC} was well below 1%; (2) a controlled .6% variation in V_{DC} was available by using the bridge circuit meter; (3) The maximum long term variations in V_{DC} were no more than 1%.

Using this knowledge, the next step was to measure how this variation in V_{DC} was related to variations in the klystron pulse amplitude, without de-Q'ing. An attenuated sample of the klystron pulse was fed into a Tektronix Type-Z plug-in unit of the oscilloscope. The Z-module is a differential comparator which allows one to measure very small fluctuations in amplitude by biasing out the main body of the waveform and turning the sensitivity up as high as desired. The dc voltage was set at a nominal 15kV, and the klystron pulse appeared on the scope as 50 volts in amplitude. After biasing out the main part of the klystron pulse, sensitivity was set at .1volt/cm, and the following data was noted:

amplitude jitter = .6 volts,

change in amplitude = \pm .6 volts as V_{DC} was varied by \pm .6%.

Therefore, the percentage of fluctuation in pulse amplitude caused by .6% variation in V_{DC} was $(.6/50) \times 100\% = 1.2\%$. As a guideline for later work, or as a performance measure of the prototype, a number η was defined as

$$\eta = \frac{\Delta V_{\text{pulse}}\%}{\Delta V_{DC}\%},$$

and for the system without de-Q'ing, this number was found to be 2. Later, the true worth of the prototype was judged by calculating the new η , and comparing it with 2.

B. TESTING OF THE PROTOTYPE

When the prototype was first installed, a number of minor modifications had to be made to the prototype and to the interface between the prototype and the original modulator. Some of these changes were necessary before the regulation could even be measured. These are discussed below as preliminary changes. Other changes were made but these were not necessary to the completion of the testing. These are entitled, simply "other changes". Finally, the regulation and effect of the prototype on the beam intensity are discussed.

1. Preliminary Problems and Circuit Changes

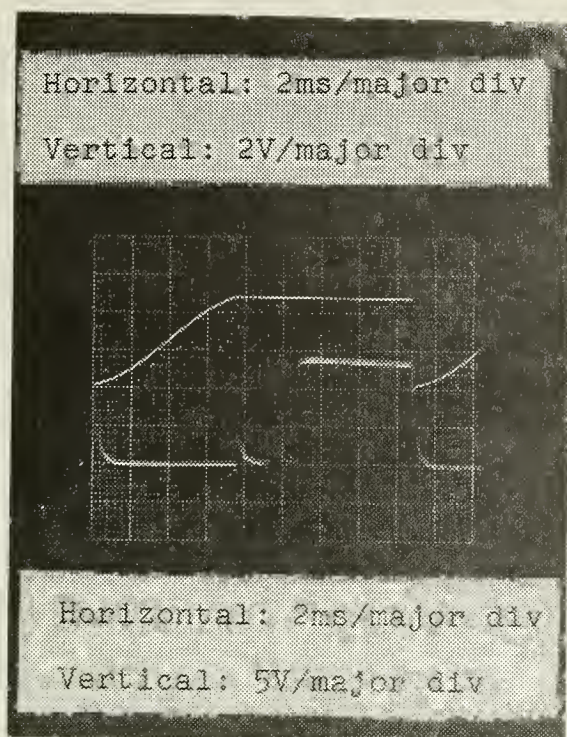
After the prototype was installed, the first thought was to use the previously described test and use η as a

criterion in adjusting for the optimum value of C_2 in the compensated divider. However, early in the testing stage, the compensated divider began to malfunction, causing a large number of problems including excessive loading of the dc power supply of Fig. 1, extreme overcurrents in the input transformers, erratic firing of main thyatron, and higher input signals to the comparator than the operational amplifier could handle. The compensated divider was removed, and the sampled PFN voltage was obtained instead from a resistive string already in place and used in conjunction with the main thyatron. There are seventy-two $560k\Omega$ resistors on the string, which amounts to approximately forty $M\Omega$. The output resistor for the string was then selected to be $6.3k\Omega$ and this resistor was hand-picked and measured on a bridge. With this value inserted, a PFN voltage of $38kV$ would correspond to an input of 6 volts to the comparator.

After these changes were made, there was still a major problem which inhibited system performance. When the de-Q'ing thyatron fired, it generated a huge spike which was being picked up in the grid of the main firing thyatron. This thyatron, which discharges the PFN, is normally fired by a clocked trigger every $16.7ms$. The stray pulse generated by the de-Q'ing thyatron was causing the PFN to be discharged more often than 60 times per second. As the repetition rate was altered, so was the average current in the klystron pulse. This problem was solved after the stray

pulse was traced to the grid of the main thyatron. It was found that the extra firing could be stopped by placing a small capacitance across the grid of the main thyatron. Since the pulse was nanoseconds in duration, even a very small capacitor would shunt it away from the grid. The value that worked was .001 μ f. Two 500pf 30kV capacitors were placed in parallel from the main thyatron firing grid to ground, and the problem was eliminated.

Another problem which was less serious did indicate that the choice of the operational amplifier for the comparator circuit was more important than had been expected. It was more noticeable while observing the comparator output waveform while the circuit was de-Q'ing. As shown in Chapter II, the expected comparator output was as shown in Fig. 19(b). However, Fig. 19(a) is an actual waveform observed out of the comparator while the top waveform (sampled PFN voltage) is being clipped. Note the initial spike and then the later steady high level of comparator output. With the μ 709 op-amp in the comparator, this type of output and variations of it were observed. A closer look at the sampled PFN revealed that a very large nanosecond pulse was superimposed on the charge waveform at the instant that the de-Q'ing thyatron fires. This is obviously the same pulse which had been successfully shunted from the firing grid. The pulse, occurring microseconds after the comparator initially turns on, causes the comparator output to go low again. Later, the sampled PFN voltage rises above the



(a) top: sampled PFN voltage

bottom: comparator output using $\mu 709$ op amp

(b) top: same as (a)

bottom: ideal comparator output; output using $\mu 741$ op amp

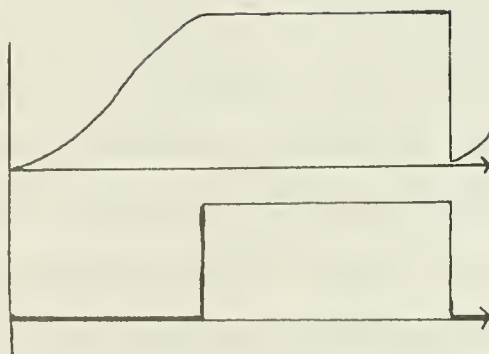


Figure 19. Clipped Charge Waveform and Comparator Output

reference level again and the comparator output goes high again until the end of the cycle.

In order to clean up the comparator output waveform, a filter was needed to block out the high nanosecond pulse. The 709 op-amp requires external frequency compensation. Without it, the op-amp responds to any stray pulse riding on the input waveform. The 741, however, is internally frequency-compensated, and when this op-amp was used, the comparator output was as expected and is shown in Fig. 19(b).

The reference voltage was designed to be variable between 4 and 6 volts, which would allow a range of over twelve kilovolts for de-Q'ing. However, the lower limit of the firing voltage of the comparator was found to be around 5 volts after the system was connected up. That is, the reference voltage setting seemed to shift by at least one volt. The actual voltage at the inverting input of the op-amp, however, was measured between 4 and 6 volts as the wiper of the potentiometer was varied over its full range. A possible explanation, based on a similar experience, is that the input legs of the op-amp inadvertently made contact, allowing the input voltage from the resistive divider to influence the reference voltage dialed in with the potentiometer. The problem was not so serious, however, because the normal operating V_{DC} used is around 18kV, and by raising this slightly, the higher PFN voltage can be clipped over an adequate range (upper 10%) with the reference voltage

range as high as it is. In other words, there is really no need for a reference voltage below 5 volts anyway.

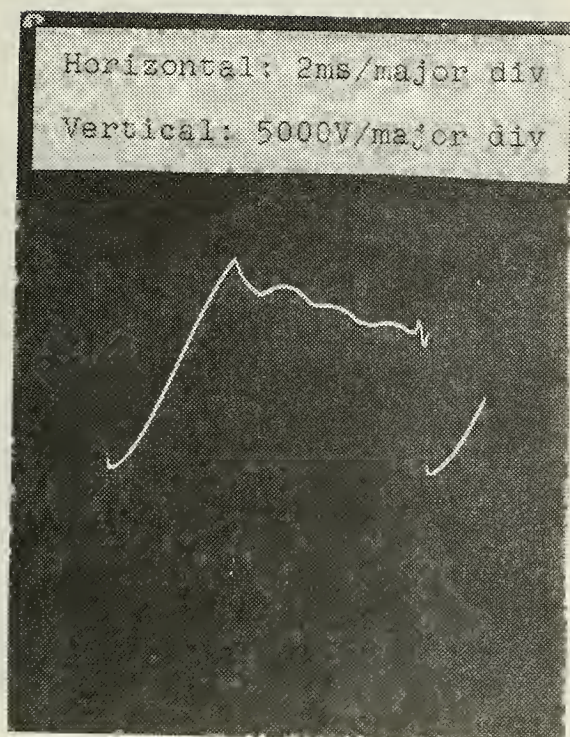
2. Other Circuit Changes

Another small change was made during the testing phase. A small choke, estimated (but not measured) to be less than $100\mu\text{H}$, was placed between the charging diodes and the PFN. It was wound in fifteen turns of hollow copper tubing around an air core about four inches in diameter, with about one-half inch between each winding. The purpose of this coil was to help reduce any negative spikes generated across the PFN when the main thyatron fires and decouple them from the plate of the de-Q'ing thyatron. However, no quantitative measurements were made to determine the effect of this choke on the system.

To see the effect of varying the capacitance of the de-Q'ing branch, the two 16kV capacitors were placed in their three possible configurations and the average current in the thyatron I_{sw} (AV) was measured, and the waveform $V_{\text{DC}} + v_{\text{L}}$, i.e., the voltage on the anode of the charge diodes was recorded. The results are given in Figs. 20 and 21. It was decided to use $C = .5\mu\text{f}$ for the remainder of the testing.

3. Measuring Improvement Factor Due to Prototype

Next, a measure of η was made with the prototype installed, just to see how "good" the de-Q'ing was. V_{DC} was changed from 17.5kV to 20kV. This is a percentage fluctuation of $2.5(100)/18.75 = 13.3\%$. This caused the klystron



(a) De-Q'ing $C = .25\mu\text{f}$
 $R = 5\text{k}\Omega$
 Average current = 200ma

(b) De-Q'ing $C = 1.0\mu\text{f}$
 $R = 5\text{k}\Omega$
 Average current = 200ma

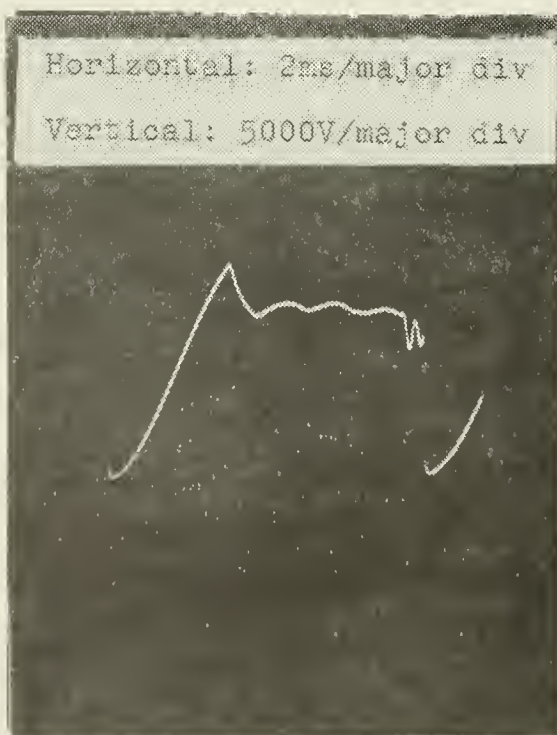
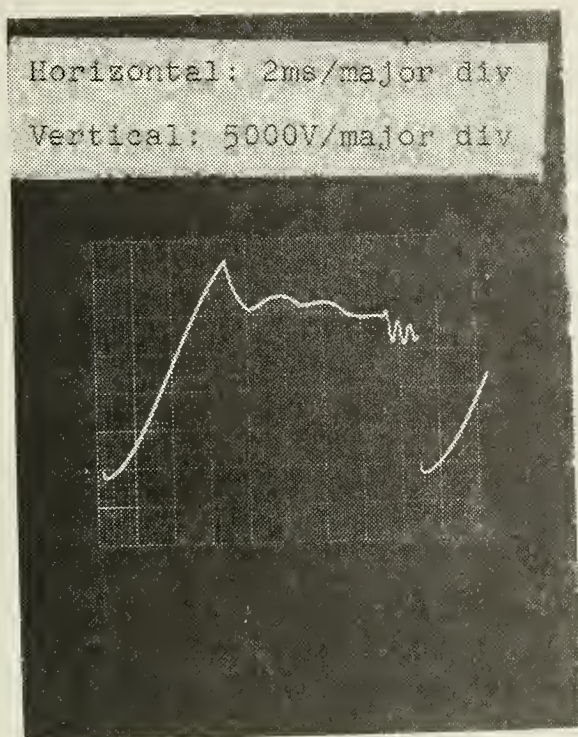


Figure 20. $V_{\text{DC}} + v_L$ for Different Values of C



(a) Actual waveform at
anode of charge diodes

$$R = 5k\Omega$$

$$C = .5\mu f$$

$$\text{Average current} = 225 \text{ ma}$$

(b) Theoretical waveform at
anode of charge diodes

$$R = 5k\Omega$$

$$C = .5\mu f$$

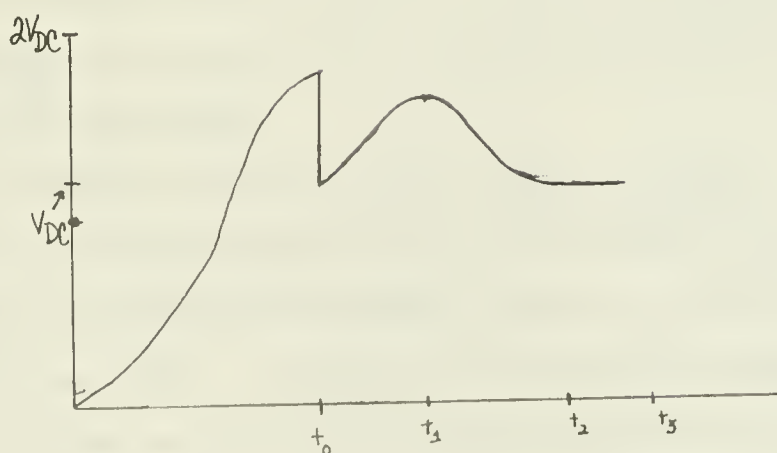


Figure 21. $V_{DC} + v_L$ for $C = .5\mu f$

pulse to vary in amplitude by .13 volts out of 44, or .3%. Thus, the value of η with the prototype installed is $3/133 = .026$. This is 77 times better regulation than that observed prior to installation.

Further improvement was obtained by employing a very simple form of resistive compensation, which is described in Appendix B. It involved a change in the circuit, and the final overall complete circuit diagram is given in Fig. 22. When this configuration was tested for regulation, the following was observed. When V_{DC} was varied by 10.5%, the klystron pulse amplitude varied by only $.05/40 = .125\%$. Thus, the new value of η is $.125/10.5 = .0119$. This is 168 times better regulation than that observed prior to installation.

The final test of the new prototype was made to determine (1) how beam intensity (current) varied as a function of klystron voltage and (2) how the V_{DC} fluctuations which had formerly caused beam to be lost affected the beam with the prototype operating.

The dc voltage was set at $.74 \times 25\text{kV}$ or 18.5kV, and the de-Q'ing reference adjusted to clip the upper 3%. The klystron pulse exhibited amplitude jitter of less than .1 volt out of 50, or .2%. To reduce the jitter the heater and reservoir voltage on the de-Q'ing thyatron were raised slightly until the purple glow of the thyatron became steady. This reduced the jitter in the klystron pulse to less than $.02/50 = .04\%$.

The rf was adjusted in frequency and amplitude until a suitable maximum beam intensity was observed. The de-Q'ing reference voltage was decreased until the beam intensity had decreased to one half the original value, and the percentage change in klystron voltage was recorded as -1%. The de-Q'ing reference was then increased until the beam intensity passed through its maximum and fell to one-half the maximum. Again the percentage change in klystron voltage was recorded as +1% above the setting where the beam current was maximum. Thus, as shown in Fig. 23 in simple form, a 2% range of de-Q'ing corresponds to a variation over a large portion of the beam intensity. So, really, only a very small range of de-Q'ing is actually necessary. Because the klystron focusing coils are tuned at a certain voltage, and must remain as close as possible to this voltage in order to present a constant impedance, the de-Q'ing circuitry will always be operating at the same nominal voltage (about 18.5kV for V_{DC}) and it will only be necessary to vary the reference voltage a few percent.

Finally, the dc input voltage was varied by $\pm .6\%$ as discussed at the beginning of this chapter. It was known that prior to installation of the prototype, this very change always caused the beam intensity to drop to zero (beam loss). However, with the prototype in place, this fluctuation had no noticeable effect on the beam intensity.

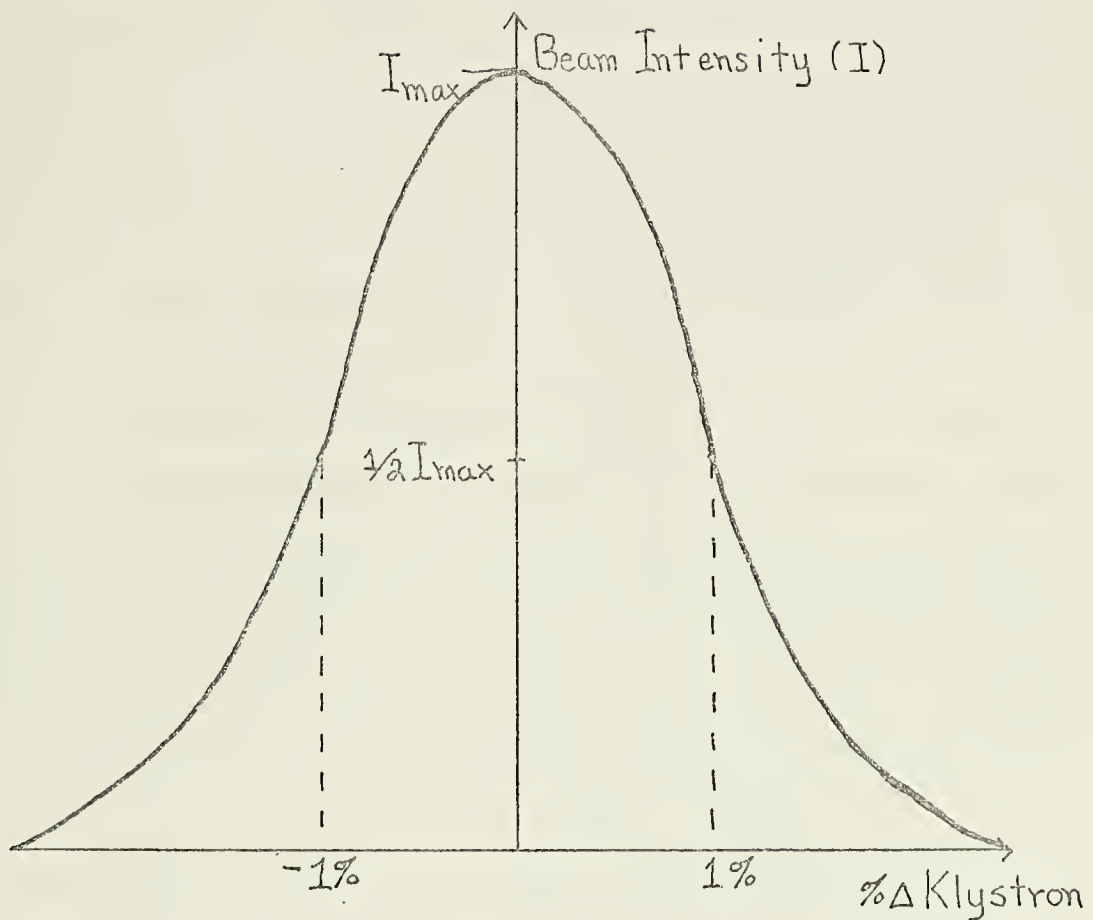


FIGURE 23-SIMPLE DIAGRAM OF
RELATIONSHIP OF BEAM INTENSITY
TO KLYSTRON VOLTAGE

APPENDIX A

Derivation of Equation (8)

Beginning with Fig. 6(b), the equivalent circuit for the de-Q'ing path, one first determines the conditions of the circuit at time t_0 , the instant that the switch is closed. The capacitor was uncharged before t_0 and the voltage across a capacitor cannot change instantaneously. Since all three elements are connected in shunt, $v_C(t) = v_L(t) = v_R(t)$ and $v_L(t_0) = v_C(t_0) = 0$.

By assumption the current flowing in the choke was I_0 in the direction shown just prior to t_0 . According to the sign convention indicated in the figure, this must be considered as $-I_0$. Since current through a choke cannot be changed instantaneously, $i_L(t_0) = -I_0$. In terms of $v_C(t_0)$, since initially all current in the circuit flows through C, this can be written as $\dot{v}_C(t_0) = I_0/C = \dot{v}_L(t_0)$.

With these conditions in mind, one first writes Kirchhoff's current law as

$$i_L + i_C + i_R = 0$$

which, in terms of v_L , becomes

$$i_L(t_0) + \frac{1}{L} \int_{t_0}^t v_L(\tau) d\tau + \frac{1}{R} v_L(t) + C \frac{dv_L}{dt} = 0$$

Differentiating the above equation and some manipulation yields

$$\ddot{v}_L + \frac{1}{RC} \dot{v}_L + \frac{1}{LC} v_L = 0.$$

At this point it is convenient to take the Laplace transform of the above equation. Letting $V(s) = L\{v_L(t)\}$ one obtains

$$V(s) = \frac{\frac{I_0}{C}}{s^2 + \frac{s}{RC} + \frac{1}{LC}}.$$

For the damped oscillatory case which is used in the text, this can be written as

$$V(s) = \frac{\frac{I_0}{C}}{\left[s + \frac{1}{2RC}\right]^2 + \left[\frac{1}{LC} - \frac{1}{4R^2C^2}\right]}$$

Letting $\omega_0 = \sqrt{(1/LC) - (1/4R^2C^2)}$ and taking the inverse transform, one obtains

$$v_L(t) = \frac{I_0}{C\omega_0} e^{-(t-t_0)/2RC} \sin \omega_0(t-t_0).$$

Multiplying the numerator and demonimator of the term in the exponent by ω_0 gives

$$v_L(t) = \frac{I_0}{\omega_0 C} e^{-\omega_0(t-t_0)/2\omega_0 RC} \sin \omega_0(t-t_0)$$

which is exactly Eq. (8) in the text.

APPENDIX B

Alternative Method of Compensation

Figure 24 shows the effect of a shift in V_{DC} on a system with a constant delay τ . In the first case, the voltage level at which the command to regulate is given, v_s is held constant. This means that the times t_1 and t_2 when the command is given are different. They are related by the equation

$$v_s = V_{DC}(1 - \cos \omega t_1) = (1+x)V_{DC}(1 - \cos \omega t_2) .$$

For a given t_1 and V_{DC} and v_s and percentage change x , t_2 could be calculated. Then an expression could be obtained for the error in the firing voltage, Δv_{PFN} .

$$\Delta v_{PFN} = (1+x)V_{DC}(1 - \cos \omega(t_2 + \tau)) - V_{DC}(1 - \cos \omega(t_1 + \tau)) .$$

To calculate Δv_{PFN} one must know the value of τ . This of course can be estimated (in this system it is about 100 μ s) and for a given percentage shift in V_{DC} , a value for Δv_{PFN} could be found and the regulation could be calculated.

To compensate for the delay, one might reverse the procedure. For ideal regulation $\Delta v_{PFN} = 0$. Starting with this condition, one can obtain an expression for t_2 as a function of t_1 , x , and τ . Then as shown in the second case in the figure, the voltage level at which the command to regulate is given would no longer be constant. In fact, one can

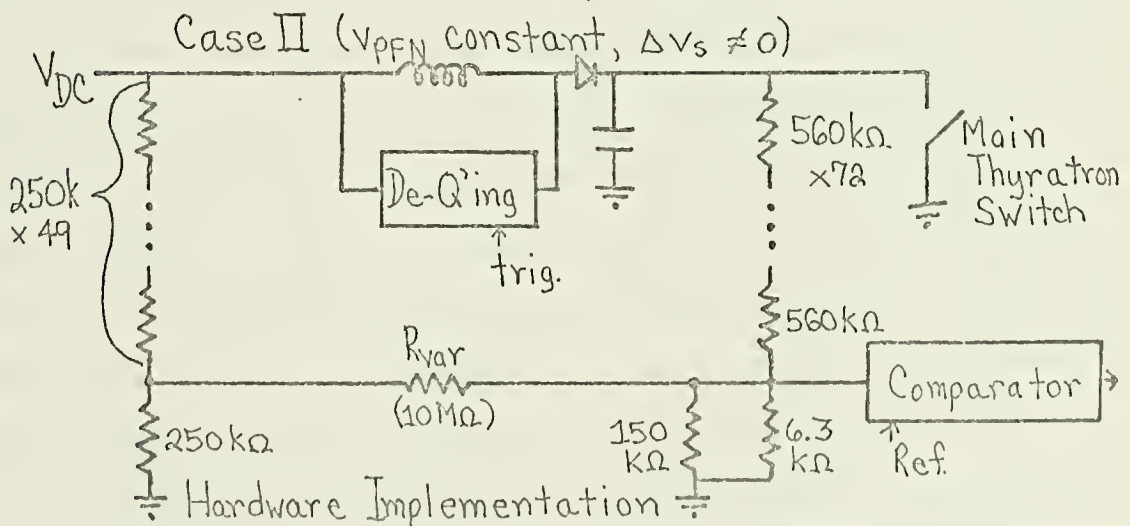
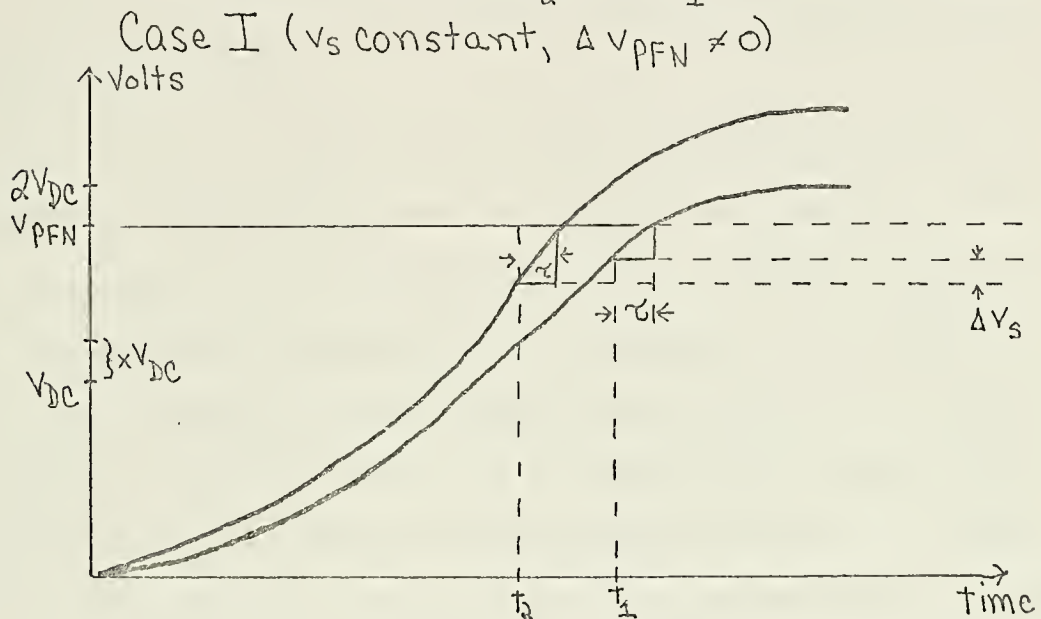
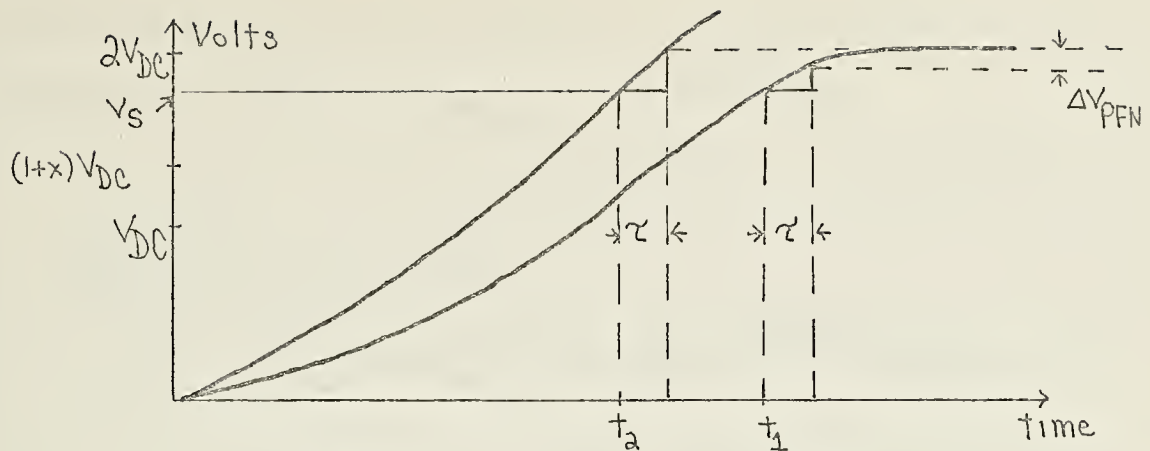


FIGURE 24-EXPLANATION OF ALTERNATE TYPE OF COMPENSATION

write an expression for the amount of shift that would be necessary to achieve $\Delta v_{\text{PFN}} = 0$. It would be

$$\Delta v_s = V_{\text{DC}}(\lambda - \cos \omega t_1 - \lambda + \cos \omega t_2 - x + x \cos \omega t_2).$$

This can be written as

$$\Delta v_s = (x(\cos \omega t_2 - 1) + \cos \omega t_2 - \cos \omega t_1)V_{\text{DC}}$$

or

$$\Delta v_s = K(x, \tau)V_{\text{DC}}.$$

This equation implies that better regulation can be achieved by varying the level at which the command to regulate is given, v_s , by an amount which is proportional to V_{DC} . The factor of proportionality depends on the delay and on how much V_{DC} varies and in general is difficult to calculate. However, using this principle, Δv_s can be made dependent on V_{DC} by the circuitry shown in Fig. 24. This is the configuration which provided the improvement mentioned in the final section of the text. The value of R_{var} was $10\text{M}\Omega$ and the extra shunt resistor ($150\text{k}\Omega$) was used to achieve $\eta = .0119$, but had time permitted (and this will most likely be done if better regulation is ever desired), the value of R_{var} could have been experimentally varied and correlated with η . The values given, however, were more than adequate for the present uses of the circuit. It seems as though this method of experimentally determining the percentage of V_{DC} to feed into the sample is much easier than to try to calculate it using the equations.

BIBLIOGRAPHY

1. Hydrogen Thyratrons, English Electric Valve Co. Ltd., June 1964.
2. Stanford University Microwave Laboratory Report 173, Pulsers for the Stanford Linear Electron Accelerator, by P.A. Pearson, November, 1952.
3. Neal, R.B., and others, eds., The Stanford Two Mile Linear Accelerator, pp. 411-437, W.A. Benjamin, Inc., 1968.

INITIAL DISTRIBUTION LIST

	No. Copies
1. Defense Documentation Center Cameron Station Alexandria, Virginia 22314	2
2. Library, Code 0212 Naval Postgraduate School Monterey, California 93940	2
3. Dr. G.D. Ewing, Code 52Ew Naval Postgraduate School Monterey, California 93940	2
4. E.B. Dally, Code 61DD Naval Postgraduate School Monterey, California 93940	5
5. ENS Ralph D. Skiano, USN 114 N. 4th St. Darby, Pennsylvania 19023	1
6. Department of Electrical Engineering, Code 52 Code 52, Monterey, California 93940	1
7. F.R. Buskirk, Code 61Bs Naval Postgraduate School Monterey, California 93940	1
8. William T. Tomlin Stanford Linear Accelerator Center, Stanford University PO Box 4349 Stanford, California 94305	1

DOCUMENT CONTROL DATA - R & D

(Security classification of title, body of abstract and indexing annotation must be entered when the overall report is classified)

1. ORIGINATING ACTIVITY (Corporate author)

Naval Postgraduate School
Monterey, California 93940

2a. REPORT SECURITY CLASSIFICATION

Unclassified

2b. GROUP

3. REPORT TITLE

Design, Construction and Testing of a High Voltage Pulsed Regulator
for Use in the NPS Linear Accelerator

4. DESCRIPTIVE NOTES (Type of report and inclusive dates)

Master's Thesis; June 1973

5. AUTHOR(S) (First name, middle initial, last name)

Ralph Dennis Skiano

6. REPORT DATE

June 1973

7a. TOTAL NO. OF PAGES

87

7b. NO. OF REFS

3

8a. CONTRACT OR GRANT NO.

8b. ORIGINATOR'S REPORT NUMBER(S)

b. PROJECT NO.

c.

9b. OTHER REPORT NO(S) (Any other numbers that may be assigned
this report)

d.

10. DISTRIBUTION STATEMENT

Approved for public release; distribution unlimited.

11. SUPPLEMENTARY NOTES

12. SPONSORING MILITARY ACTIVITY

Naval Postgraduate School
Monterey, California 93940

13. ABSTRACT

This paper describes the design, construction and testing of a pulsed high voltage regulator installed in one modulator of the Naval Postgraduate School Linear Accelerator. The design is adapted from a similar network in use at Stanford University. The prototype system was found to improve the voltage regulation by a factor of 168, and to eliminate undesirable energy shifts in the electron beam due to fluctuations in line voltage.

KEY WORDS

LINK A

LINK B

LINK C

ROLE

WT

ROLE

WT

ROLE

WT

De-Q'ing

High Voltage

Linear accelerator

Pulsed regulator

Thesis

S5465

Skiano

145185

c.1

Design, construction
and testing of a high
voltage pulsed regulator
for use in the NPS linear
accelerator.

thesS5465

Design, construction and testing of a hi



3 2768 001 00603 4

DUDLEY KNOX LIBRARY